0616 E.P.H.), the Jain Foundation (E.P.H.), the Crystal Ball of Virginia Beach (Muscular Dystrophy Association USA) (E.P.H.), the National Center for Medical Rehabilitation Research 5R24HD050846-02 (E.P.H.), the NIH Wellstone Muscular Dystrophy Research Centers 1U54HD053177-01A1 (E.P.H.), and the Ministry of Health, Labor, and Welfare of Japan (Research on Nervous and Mental Disorders, 16B-2, 19A-7; Health and Labor Sciences, Research Grants for Translation Research, H19-translational research-003, Health Sciences Research Grants for Research on Psychiatry and Neurological Disease and Mental Health, H18-kokoro-019) (S.T.).

We thank Drs S. Duguez, J. Nazarian, H. Gordish-Dressman, Y. Aoki, T. Saito, K. Yuasa, N. Yugeta, S. Ohshima, Z.-H. Shin, MR. Wada, K. Fukushima, S. Masuda, K. Kinoshita, H. Kita, S. Ichikawa, Y. Yahata, T. Nakayama, A. Rabinowitz, and JR. Beauchamp for discussions and technical assistance.

References

1. Hoffman EP, Brown RH Jr, Kunkel LM. Dystrophin: the protein product of the Duchenne muscular dystrophy locus. Cell 1987;51:919–928.
2. Matsumura K, Campbell KP. Dystrophin-glycoprotein complex: its role in the molecular pathogenesis of muscular dystrophies. Muscle Nerve 1994;17:2–15.
3. Koenig M, Beggs AH, Moyer M, et al. The molecular basis for Duchenne versus Becker muscular dystrophy: correlation of severity with type of deletion. Am J Hum Genet 1989;45:498–506.
4. England SB, Nicholson LV, Johnson MA, et al. Very mild muscular dystrophy associated with the deletion of 46% of dystrophin. Nature 1990;343:180–182.
5. Dunckley MG, Manoharan M, Villiet P, et al. Modification of splicing in the dystrophin gene in cultured Mdx muscle cells by antisense oligoribonucleotides. Hum Mol Genet 1998;7: 1083–1090.
6. van Deutekom JC, Janson AA, Ginjaar IB, et al. Local dystrophin restoration with antisense oligonucleotide PRO051. N Engl J Med 2007;357:2677–2686.
7. Yokota T, Duddy W, Partridge T. Optimizing exon skipping therapies for DMD. Acta Myol 2007;26:179–184.
8. Aartsma-Rus A, Janson AA, Kaman WE, et al. Antisense-induced multiexon skipping for Duchenne muscular dystrophy makes more sense. Am J Hum Genet 2004;74:83–92.
9. Sharp NJ, Kornegay JN, Van Camp SD, et al. An error in dystrophin mRNA processing in golden retriever muscular dystrophy, an animal homologue of Duchenne muscular dystrophy. Genomics 1992;13:115–121.
10. McClorey G, Moulton HM, Iversen PL, et al. Antisense oligonucleotide-induced exon skipping restores dystrophin expression in vitro in a canine model of DMD. Gene Ther 2006; 13:1373–1381.
11. Shimatsu Y, Katagiri K, Furuta T, et al. Canine X-linked muscular dystrophy in Japan (CXMDJ). Exp Anim 2003;52:93–97.
12. Summerton J, Weller D. Morpholino antisense oligomers: design, preparation, and properties. Antisense Nucleic Acid Drug Dev 1997;7:187–195.
13. Yokota T, Takeda S, Lu QL, et al. A renaissance for anti-sense oligonucleotide drugs in neurology: exon-skipping breaks new ground. Arch Neurol 2009;66:32–38.
14. Jankowski RJ, Haluszczak C, Trucco M, Huard J. Flow cytometric characterization of myogenic cell populations obtained via the preplate technique: potential for rapid isolation of muscle-derived stem cells. Hum Gene Ther 2001;12:619–628.
15. Yokota T, Lu QL, Morgan JE, et al. Expansion of revertant fibers in dystrophic mdx muscles reflects activity of muscle precursor cells and serves as an index of muscle regeneration. J Cell Sci 2006;119:2679–2687.
16. Abramoff MD, Magelhaes PJ, Ram SJ. Image processing with ImageJ. Biophotonics Int 2004;11:36–42.
17. Araishi K, Sasaoka T, Imamura M, et al. Loss of the sarcoglycan complex and sarcospan leads to muscular dystrophy in beta-sarcoglycan-deficient mice. Hum Mol Genet 1999;8:1589–1598.
18. Shimatsu Y, Yoshimura M, Yuasa K, et al. Major clinical and histopathological characteristics of canine X-linked muscular dystrophy in Japan, CXMDJ. Acta Myol 2005;24:145–154.
19. Alter J, Lou F, Rabinowitz A, et al. Systemic delivery of morpholino oligonucleotide restores dystrophin expression bodywide and improves dystrophic pathology. Nat Med 2006;12:175–177.
20. Reiss J, Rininsland F. An explanation for the constitutive exon 9 cassette splicing of the DMD gene. Hum Mol Genet 1994; 3:295–298.
21. Aartsma-Rus A, De Winter CL, Janson AA, et al. Functional analysis of 114 exon-internal AONs for targeted DMD exon skipping: indication for steric hindrance of SR protein binding sites. Oligonucleotides 2005;15:284–297.
22. Yoshimura M, Sakamoto M, Ikemoto M, et al. AAV vector-mediated microdystrophin expression in a relatively small percentage of mdx myofibers improved the mdx phenotype. Mol Ther 2004;10:821–828.
23. Liang KW, Nishikawa M, Liu F, et al. Restoration of dystrophin expression in mdx mice by intravascular injection of naked DNA containing full-length dystrophin cDNA. Gene Ther 2004;11:901–908.
24. Yokota T, Pistilli E, Duddy W, Nagaraju K. Potential of oligonucleotide-mediated exon-skipping therapy for Duchenne muscular dystrophy. Exp Opin Biol Ther 2007;7:831–842.
25. Yugeta N UN, Fujii Y, Yoshimura M, et al. Cardiac involvement in Beagle-based canine X-linked muscular dystrophy in Japan (CXMDJ): electrocardiographic, echocardiographic, and morphologic studies. BMC Cardiovasc Disord 2006;6:47.
26. Jearawiriyapaisarn N, Moulton HM, Buckley B, et al. Sustained dystrophin expression induced by peptide-conjugated morpholino oligomers in the muscles of mdx mice. Mol Ther 2008;16: 1624–1629.
27. Vannan M, McCreery T, Li P, et al. Ultrasound-mediated transfection of canine myocardium by intravenous administration of cationic microbubble-linked plasmid DNA. J Am Soc Echocardiogr 2002;15:214–218.
28. Fall AM, Johnsen R, Honeyman K, et al. Induction of revertant fibres in the mdx mouse using antisense oligonucleotides. Genet Vaccines Ther 2006;4:3.
29. Aartsma-Rus A, Janson AA, van Ommen GJ, van Deutekom JC. Antisense-induced exon skipping for duplications in Duchenne muscular dystrophy. BMC Med Genet 2007;8:43.
30. Aartsma-Rus A, Kaman WE, Weij R, et al. Exploring the frontiers of therapeutic exon skipping for Duchenne muscular dystrophy by double targeting within one or multiple exons. Mol Ther 2006;14:401–407.
31. Nakamura A, Yoshida K, Fukushima K, et al. Follow-up of three patients with a large in-frame deletion of exons 45-55 in the Duchenne muscular dystrophy (DMD) gene. J Clin Neurosci 2008;15:757–763.
32. Beroud C, Tuffery-Giraud S, Matsuo M, et al. Multiexon skipping leading to an artificial DMD protein lacking amino acids from exons 45 through 55 could rescue up to 63% of patients with Duchenne muscular dystrophy. Hum Mutat 2007;28:196–202.

Journal of Human Genetics (2009), 1–4

www.nature.com/jhg

SHORT COMMUNICATION

Characterization of deletion breakpoints in patients with dystrophinopathy carrying a deletion of exons 45–55 of the Duchenne muscular dystrophy (DMD) gene

Daigo Miyazaki[1], Kunihiro Yoshida[1], Kazuhiro Fukushima[1], Akinori Nakamura[1,2], Kayo Suzuki[3], Toshiyuki Sato[4], Shin'ichi Takeda[2] and Shu-ichi Ikeda[1]

Deletion of exons 45–55 (del45–55) in the Duchenne muscular dystrophy gene (*DMD*) has gained particular interest in the field of molecular therapy, because it causes a milder phenotype than DMD, and therefore, may represent a good candidate for the goal of a multiple exon-skipping strategy. We have precisely characterized deletion breakpoints in three patients with del45–55 in *DMD*. Two of them were young adult males of the X-linked dilated cardiomyopathy phenotype, and the third patient revealed the mild Becker muscular dystrophy phenotype of late onset. The deletion breakpoints differed among patients. The deletion started at nt 226 604, 231 518, 117 284 in intron 44, and ended at nt 64 994, 59 314, 71 806 in intron 55, respectively. Deletion junctions showed no significant homology between the sequences adjacent to the distal and proximal end joints in these patients. Deletion breakpoints were not primarily associated with any particular sequence element, or with a matrix attachment region. However, there were several palindromic sequences and short tandem repeats at or near the breakpoints. These sequences, with a marked propensity to form secondary DNA structure intermediates, may predispose local DNA to breakage and intragenic recombination in these patients.
Journal of Human Genetics advance online publication, 9 January 2009; doi:10.1038/jhg.2008.8

Keywords: breakpoint; deletion; Duchenne muscular dystrophy (DMD); dystrophin; genomic sequence; X-linked dilated cardiomyopathy (XLDCM)

INTRODUCTION

The Duchenne muscular dystrophy gene (*DMD*) is the largest one so far identified, spanning more than 2.5 Mb and occupying roughly 0.1% of the human genome.[1] Mutations in *DMD* cause a devastating muscular dystrophy named Duchenne/Becker muscular dystrophy (DMD/BMD). The cardio-specific phenotype of dystrophinopathy is also known as X-linked dilated cardiomyopathy (XLDCM).[1] Intragenic deletions and duplications together account for over two-thirds of the mutations found in DMD/BMD patients.[2–7] Despite heterogeneity in both deletion size and location, two deletion 'hotspots' have been identified in *DMD*: a minor 'hotspot' including exons 2–19, and the major one involving exons 40–50 or 45–55.[2,4,5,7]

Among deletions of variable sizes and locations found in DMD/BMD patients, deletion of exons 45–55 (del45–55) in *DMD* has gained particular attention because an artificial dystrophin with del45–55 created by a multiple exon-skipping strategy could transform the DMD phenotype into the asymptomatic or milder BMD phenotype.[8] We reported three patients with del45–55 who presented with the phenotypes far from DMD.[9] Two of them were young adult males of the XLDCM phenotype.[9,10] The third patient revealed the mild BMD phenotype of late onset.[9,11] Our patients support the hypothesis that del45–55 could be a good candidate for the goal of a multiple exon-skipping strategy for DMD.

To elucidate the molecular basis of del45–55 in more detail, we have characterized the breakpoints of del45–55 in *DMD* in these three patients. To our knowledge, only two breakpoints have been precisely described in intron 44,[12] which is the major deletion-prone region in *DMD*.[1,6,7,13] On the other hand, an analysis of breakpoints in intron 55 has never been reported.

[1]Department of Medicine (Neurology and Rheumatology), Shinshu University School of Medicine, Nagano, Japan; [2]Department of Molecular Therapy, National Institute of Neuroscience, National Center of Neurology and Psychiatry, Tokyo, Japan; [3]Department of Instrumental Analysis, Research Center for Human and Environmental Science, Shinshu University, Matsumoto, Japan and [4]Science Solutions Division, Mizuho Information and Research Institute, Tokyo, Japan
Correspondence: Dr K Yoshida, Department of Medicine (Neurology and Rheumatology), Shinshu University School of Medicine, 3-1-1 Asahi, Matsumoto, Nagano 390-8621, Japan.
E-mail: kyoshida@shinshu-u.ac.jp
Received 18 September 2008; revised 6 November 2008; accepted 7 November 2008

MATERIALS AND METHODS

Patients

Clinical details of the patients were reported earlier.[9–11] The patient number in this study corresponded to that in the previous report.[9] Patients 1 and 2 shared the similar clinical phenotype of XLDCM. They had been free of muscular symptoms before they developed congestive heart failure along with cold-like symptoms at the age of 26 and 36 years, respectively.[9,10] Despite no obvious muscular atrophy or weakness, the hyperCKemia reminded us of dystrophinopathy. Patient 3 showed the mild BMD phenotype with muscular atrophy and weakness in the extremities, which began around the age of 59 years.[9,11] He showed no obvious cardiac involvement.

Identification of breakpoints

The sequences of introns 44 and 55 were derived from the University of California Santa Cruz (UCSC) human genome website (http://genome.ucsc.edu). The nucleotide numbering was started from the first nucleotide for each intron in this paper. A total of 53 primer sets were designed to roughly span introns 44 (28 sets) and 55 (25 sets), and to yield PCR products of 200–300 bp. Using these primer sets, three patients were independently screened by PCR for the presence or absence of regions targeted by primer sets. The failure of PCR amplification indicated that either the entire fragment or at least one annealing site was deleted. PCR reaction conditions were as follows: 95 °C for 1 min (initial denaturation), 30 cycles of 95 °C for 30 s (denaturation), 60 °C for 1 min (annealing), 72 °C for 1 min (extension) and 95 °C for 7 min (final extension). When mapping of both 5′ and 3′ breakpoints was restricted to less than 1–2 kb, direct amplification was tried to obtain the junctional fragments with a combination of sense primers in intron 44 and antisense primers in intron 55. As amplification of deletion junctions always yielded a single band, the PCR products were purified and sequenced.

Intron sequence analysis

Searches for interspersed repetitive elements were performed by using the RepeatMasker program (http://repeatmasker.genome.washington.edu, http://repeatmasker.org) run under sensitive settings (we selected 'cross_match' as search engine, and 'slow' as speed/sensitivity). Matrix attachment regions (MARs) were identified by using the MAR-Wiz program (http://www.futuresoft.org/modules/MarFinder/index.html). In MAR-Wiz analysis, all the rules included in the Core MAR rules were selected. Sliding window parameters were as follows: window width 1000, slide distance 100, cutoff threshold 0.6 and run-length 3.

RESULTS

Sequence characterization of introns 44 and 55 in *DMD*

The sequences of introns 44 and 55 were first analyzed for interspersed repetitive elements, the frequency of which was 32. 7% for intron 44 and 40.5% for intron 55 (S1, Electric Supplementary material). The value for intron 55, but not for intron 44, was higher than the corresponding value for the whole *DMD* (35.6%).[14]

The distribution of repetitive elements and the possible MAR sites are schematically shown in (S2, Electric Supplementary material). There were four regions with a cutoff threshold of more than 0.6 in intron 44; they were the regions around nt 33 000 (average strength 0.658), nt 124 000 (0.715), nt 131 300 (0.749) and nt 174 800 (0.819). Those regions in intron 55 were as follows: the regions around nt 4700 (0.740) and nt 35 300 (0.758). The regions around nt 1100 in intron 44 and nt 58 200 in intron 55 were also found to have a relatively high MAR potential.

Analysis of breakpoint sequences

The sizes and breakpoints of the deletion were different in these patients (Figure 1), but the breakpoints of patients 1 and 2 were very close, relative to the large size of introns 44 and 55 (Figure 1). The deletions spanned 427.6 kb (patient 1), 417.1 kb (patient 2) and 515.5 kb (patient 3). None of the deletions affected the promoter regions and unique exon 1 of dystrophin isoforms Dp140 and Dp116, which are located in the introns 44 and 55, respectively.[15,16]

Deletion breakpoints did not appear to be preferentially associated with any particular type of repetitive elements, although three of the six breakpoints were located in LINE-1 elements (S3, Electric Supplementary material). The breakpoints in intron 44 in these patients gathered in the 3′-half of that intron (Figure 1; S2, Electric Supplementary material), as pointed out earlier.[6,12,13] Further the breakpoints in intron 55 showed a relative clustering within a region of approximately 10 kb (Figure 1; S2, Electric Supplementary material). None of the breakpoints appeared to have a close association with MAR sites.

Figure 2 shows the breakpoint sequences of the three patients compared with 40–50 bp of wild-type sequence on each side. Deletion junctions did not share a significant homology between the sequences adjacent to the distal and proximal end points in these patients. In patient 1, a 12-bp triplication was found at the breakpoint. The sequence TTTAAA, which is known to be capable of inducing a curvature of DNA, was present near the breakpoints of both introns 44 and 55 in patient 1 (Figure 2). Short (6–9 bp) tandem repeats were observed at or near the breakpoints in patients 1 and 2 (Figure 2). Palindromic sequences with 6 or more base pairs were found near the breakpoints in patient 1 (Figure 2). The 7-bp complementary sequences that flanked the breakpoint were found in intron 44 in patient 3.

DISCUSSION

In this report, we have precisely characterized the breakpoints in three patients with del45–55 in *DMD*. We have detected no substantial homologies between the normal DNA sequences located across the breakpoints in introns 44 and 55. One of the breakpoints was located in LINE-1 repetitive elements in all patients, but the other ends were not associated with any particular repetitive elements. These observations in the patients with del45–55 are consistent with those in the cases with other types of deletion in *DMD*,[12–14,17–19] again supporting that homologous recombination is not the major cause of deletions in *DMD*.

Human gene deletions are induced by several mechanisms, the relative importance of which is probably governed by local and secondary DNA structures.[20] Krawczak and Cooper[20] have pointed out that human sequences involved in deletion events often contain a short deletion consensus sequence, TG(A/G)(A/G)(G/T)(A/C), and are often associated with palindromic sequences. Palindromic sequences are likely to locally induce the formation of a hairpin loop structure in a single strand of DNA, and serve as a strong topoisomerase II cleavage site.[21,22] We have identified several consensus sequences, palindromic sequences and short tandem repeats at or near the breakpoints. These sequences may promote DNA instability by facilitating the formation of secondary structure intermediates, which predispose DNA to breakage and intragenic recombination.[17,20,23]

The deletion breakpoints were different in three patients analyzed in this study; however, the breakpoints of patients 1 and 2 were in very close proximity in the relatively large introns 44 and 55. The difference of breakpoint locations between these two patients was approximately 5000 bp at both ends within introns 44 and 55. Their clinical features, compatible with XLDCM, were very similar to each other, and outstanding among dystrophinopathy. It is possible that the close similarity of clinical features and molecular defects has some pathogenic or biological significance. Some *trans*- or *cis*-acting elements that

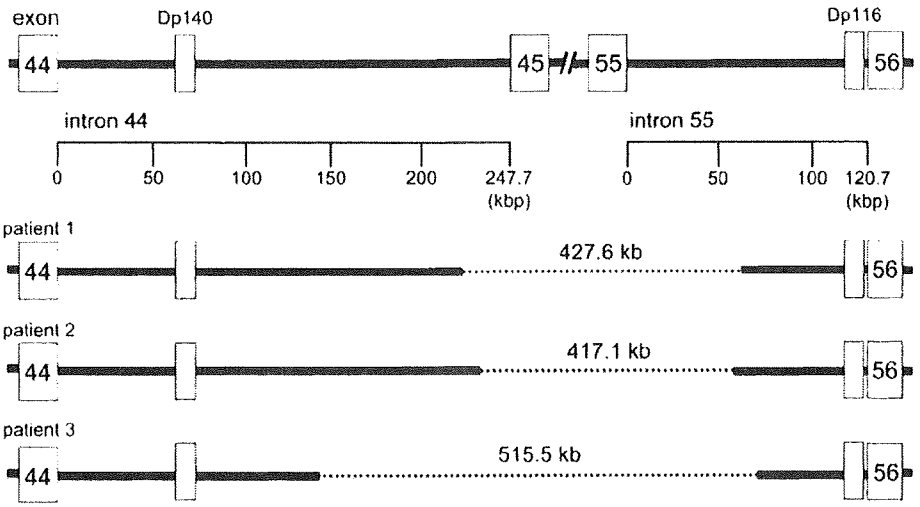

Figure 1 Schematic presentation of deletion breakpoints in three patients. The relative locations of the unique promoter and exon 1 of Dp140 and Dp116 are shown. The dotted lines indicate the deleted region in the patients.

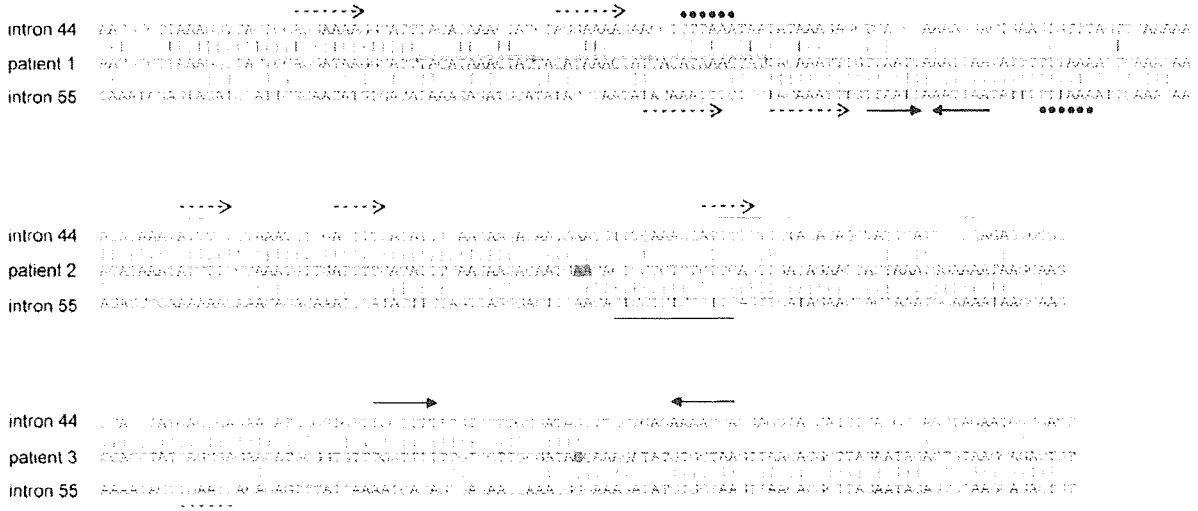

Figure 2 Genomic sequences spanning the breakpoints in three patients, with the corresponding normal intronic regions. Only the 5′–3′ strands are shown. Triplicated regions are in white boxes, and homology regions across the deletion breakpoints are in gray boxes. Arrows and dotted arrows indicate palindromic sequences with a stem of 6 or more base pairs and short tandem repeats, respectively. Lines indicate runs of consecutive pyrimidine nucleotides. Dotted lines indicate the short deletion consensus sequence, TG(A/G)(A/G)(G/T)(A/C). Dots indicate the sequence TTTAAA.

are involved in the sequence within or around the deleted regions may contribute to the pathogenesis of this unique phenotype in these patients. Accumulation of dystrophinopathy patients with del45–55 and further detailed analysis of the sequence in introns 44 and 55 will be needed to answer this hypothesis.

ACKNOWLEDGEMENTS

This study was supported by a Research Grant for Nervous and Mental Disorders (8A-2) from the Ministry of Health and Welfare.

1 Muntoni, F., Torelli, S. & Ferlini, A. Dystrophin and mutations: one gene, several proteins, multiple phenotypes. *Lancet Neurol.* **2,** 731–740 (2003).

2 Forrest, S. M., Cross, G. S., Speer, A., Gardner-Medwin, D., Burn, J. & Davies, K. E. Preferential deletion of exons in Duchenne and Becker muscular dystrophies. *Nature* **329,** 638–640 (1987).

3 Koenig, M., Hoffman, E. P., Bertelson, C. J., Monaco, A. P., Feener, C. & Kunkel, L. M. Cloning of the Duchenne muscular dystrophy (DMD) cDNA and preliminary genomic organization of the DMD gene in normal and affected individuals. *Cell* **50,** 509–517 (1987).

4 Koenig, M., Beggs, A. H., Moyer, M., Scherpf, S., Heindrich, K., Bettecken, T. *et al.* The molecular basis for Duchenne versus Becker muscular dystrophy: correlation of severity with type of deletion. *Am. J. Hum. Genet.* **45,** 498–506 (1989).

5 den Dunnen, J. T., Grootscholten, P. M., Bakker, E., Blonden, L. A., Ginjaar, H. B., Wapenaar, M. C. *et al.* Topography of the Duchenne muscular dystrophy (DMD) gene: FIGE and cDNA analysis of 194 cases reveals 115 deletions and 13 duplications. *Am. J. Hum. Genet.* **45,** 835–847 (1989).

6 Blonden, L. A., Grootscholten, P. M., den Dunnen, J. T., Bakker, E., Abbs, S., Bobrow, M. *et al.* 242 breakpoints in the 200-kb deletion-prone P20 region of the *DMD* gene are widely spread. *Genomics* **10,** 631–639 (1991).

7 Oudet, C., Hanauer, A., Clemens, P., Caskey, T. & Mandel, J. L. Two hot spots of recombination in the *DMD* gene correlate with the deletion prone regions. *Hum. Mol. Genet.* **1,** 599–603 (1992).

8 Béroud, C., Tuffery-Giraud, S., Matsuo, M., Hamroun, D., Humbertclaude, V., Monnier, N. *et al.* Multiexon skipping leading to an artificial DMD protein lacking amino acids from exons 45 through 55 could rescue up to 63% of patients with Duchenne muscular dystrophy. *Hum. Mutat.* **28,** 196–202 (2007).
9 Nakamura, A., Yoshida, K., Fukushima, K., Ueda, H., Urasawa, N., Koyama, J. *et al.* Follow-up of three patients with a large deletion of exons 45–55 in the Duchenne muscular dystrophy (*DMD*) gene. *J. Clin. Neurosci.* **15,** 757–763 (2008).
10 Tasaki, N., Yoshida, K., Haruta, S., Kouno, H., Ichinose, H., Fujimoto, Y. *et al.* X-linked dilated cardiomyopathy with a large hot-spot deletion in the dystrophin gene. *Intern. Med.* **40,** 1215–1221 (2001).
11 Yazaki, M., Yoshida, K., Nakamura, A., Koyama, J., Nanba, T., Ohori, N. *et al.* Clinical characteristics of aged Becker muscular dystrophy patients with onset after 30 years. *Eur. Neurol.* **42,** 145–149 (1999).
12 Love, D. R., England, S. B., Speer, A., Marsden, R. F., Bloomfield, J. F., Roche, A. L. *et al.* Sequences of junction fragments in the deletion-prone region of the dystrophin gene. *Genomics* **10,** 57–67 (1991).
13 Sironi, M., Pozzoli, U., Cagliani, R., Giorda, R., Comi, G. P., Bardoni, A. *et al.* Relevance of sequence and structure elements for deletion events in the dystrophin gene major hot-spot. *Hum. Genet.* **112,** 272–288 (2003).
14 Toffolatti, L., Cardazzo, B., Nobile, C., Danieli, G. A., Gualandi, F., Muntoni, F. *et al.* Investigating the mechanism of chromosomal deletion: characterization of 39 deletion breakpoints in introns 47 and 48 of the human dystrophin gene. *Genomics* **80,** 523–530 (2002).
15 Byers, T. J., Lidov, H. G. W. & Kunkel, L. M. An alternative dystrophin transcript specific to peripheral nerve. *Nat. Genet.* **4,** 77–81 (1993).
16 Lidov, H. G. W., Selig, S. & Kunkel, L. M. Dp140: a novel 140 kDa CNS transcript from the dystrophin locus. *Hum. Mol. Genet.* **4,** 329–335 (1995).
17 McNaughton, J. C., Cockburn, D. J., Hughes, G., Jones, W. A., Laing, N. G., Ray, P. N. *et al.* Is gene deletion in eukaryotes sequence-dependent? A study of nine deletion junctions and nineteen other deletion breakpoints in intron 7 of the human dystrophin gene. *Gene* **222,** 41–51 (1998).
18 Suminaga, R., Takeshima, Y., Yasuda, K., Shiga, N., Nakamura, H. & Matsuo, M. Non-homologous recombination between Alu and LINE-1 repeats caused a 430-kb deletion in the dystrophin gene: a novel source of genomic instability. *J. Hum. Genet.* **45,** 331–336 (2000).
19 Nobile, C., Toffolatti, L., Rizzi, F., Simionati, B., Nigro, V., Cardazzo, B. *et al.* Analysis of 22 deletion breakpoints in dystrophin intron 49. *Hum. Genet.* **110,** 418–421 (2002).
20 Krawczak, M. & Cooper, D. N. Gene deletions causing human genetic disease: mechanisms of mutagenesis and the role of the local DNA sequence environment. *Hum. Genet.* **86,** 425–441 (1991).
21 Froelich-Ammon, S. J., Gales, K. C. & Osheroff, N. Site-specific cleavage of a DNA hairpin by topoisomerase II. *J. Biol. Chem.* **269,** 7719–7725 (1994).
22 Robinson, D. O., Bunyan, D. J., Gabb, H. A., Temple, I. K. & Yau, S. C. A small intraexonic deletion within the dystrophin gene suggests a possible mechanism of mutagenesis. *Hum. Genet.* **99,** 658–662 (1997).
23 Spitzner, J. R., Chung, I. K. & Muller, M. T. Eukaryotic topoisomerase II preferentially cleaves alternating purine-pyrimidine repeats. *Nucleic Acids Res.* **18,** 1–11 (1990).

Supplementary Information accompanies the paper on Journal of Human Genetics website (http://www.nature.com/jhg)

MECHANISMS OF DEVELOPMENT 126 (2009) 107–116

available at www.sciencedirect.com

ScienceDirect

journal homepage: www.elsevier.com/locate/modo

Reduced proliferative activity of primary POMGnT1-null myoblasts *in vitro*

Yuko Miyagoe-Suzuki[a,*], *Nami Masubuchi*[a,b], *Kaori Miyamoto*[a,b], *Michiko R. Wada*[a], *Shigeki Yuasa*[c], *Fumiaki Saito*[d], *Kiichiro Matsumura*[d], *Hironori Kanesaki*[e], *Akira Kudo*[e], *Hiroshi Manya*[f], *Tamao Endo*[f], *Shin'ichi Takeda*[a]

[a]*Department of Molecular Therapy, National Institute of Neuroscience, National Center of Neurology and Psychiatry, 4-1-1 Ogawahigashi, Kodaira, Tokyo 187-8502, Japan*
[b]*Molecular Embryology, Department of Biosciences, School of Science, Kitasato University, Kanagawa 228-8555, Japan*
[c]*Department of Ultrastructural Research, National Institute of Neuroscience, National Center of Neurology and Psychiatry, 4-1-1 Ogawahigashi, Kodaira, Tokyo 187-8502, Japan*
[d]*Department of Neurology and Neuroscience, Teikyo University School of Medicine, 2-11-1 Kaga, Itabashi-ku, Tokyo 173-8605, Japan*
[e]*Department of Biological Information, Tokyo Institute of Technology, Yokohama 226-8501, Japan*
[f]*Glycobiology Research Group, Tokyo Metropolitan Institute of Gerontology, Foundation for Research on Aging and Promotion of Human Welfare, 35-2 Sakaecho, Itabashi-ku, Tokyo 173-0015, Japan*

ARTICLE INFO

Article history:
Received 28 May 2008
Received in revised form
6 November 2008
Accepted 2 December 2008
Available online 16 December 2008

Keywords:
POMGnT1
Muscle–eye–brain disease
Satellite cells
Skeletal muscle
α-Dystroglycan
Glycosylation
Laminin

ABSTRACT

Protein O-linked mannose β1,2-N-acetylglucosaminyltransferase 1 (POMGnT1) is an enzyme that transfers N-acetylglucosamine to O-mannose of glycoproteins. Mutations of the *POMGnT1* gene cause muscle–eye–brain (MEB) disease. To obtain a better understanding of the pathogenesis of MEB disease, we mutated the *POMGnT1* gene in mice using a targeting technique. The mutant muscle showed aberrant glycosylation of α-DG, and α-DG from mutant muscle failed to bind laminin in a binding assay. *POMGnT1*$^{-/-}$ muscle showed minimal pathological changes with very low-serum creatine kinase levels, and had normally formed muscle basal lamina, but showed reduced muscle mass, reduced numbers of muscle fibers, and impaired muscle regeneration. Importantly, *POMGnT1*$^{-/-}$ satellite cells proliferated slowly, but efficiently differentiated into multinuclear myotubes *in vitro*. Transfer of a retrovirus vector-mediated *POMGnT1* gene into *POMGnT1*$^{-/-}$ myoblasts completely restored the glycosylation of α-DG, but proliferation of the cells was not improved. Our results suggest that proper glycosylation of α-DG is important for maintenance of the proliferative activity of satellite cells *in vivo*.

1. Introduction

POMGnT1 is the glycosyltransferase that catalyzes the transfer of N-acetylglucosamine (GlcNAc) to O-mannose of glycoproteins, the second step of Ser/Thr O-mannosylation (Yoshida et al., 2001; reviewed in Endo and Toda, 2003). Mutations in the *POMGnT1* gene cause muscle–eye–brain (MEB) disease, a rare autosomal recessive disorder characterized by congenital muscular dystrophy with elevated serum creatine kinase (CK) levels, severe visual failure, and gross mental retardation (Yoshida et al., 2001).

* *Corresponding author.* Tel.: +81 42 346 1720; fax: +81 42 346 1750.
E-mail address: miyagoe@ncnp.go.jp (Y. Miyagoe-Suzuki).
0925-4773/$ - see front matter © 2008 Elsevier Ireland Ltd. All rights reserved.
doi:10.1016/j.mod.2008.12.001

α-Dystroglycan (α-DG) is a heavily glycosylated glycoprotein and a well-known substrate of POMGnT1. Dystroglycan is encoded by a single gene (*DAG1*) and is cleaved into two proteins, α-dystroglycan (α-DG) and β-dystroglycan (β-DG), by posttranslational processing (Ibraghimov-Beskrovnaya et al., 1992). DGs are central components of the dystrophin–glycoprotein complex (DGC) at the sarcolemma, and α-DG was shown to serve as a cell surface receptor for laminin (Ibraghimov-Beskrovnaya et al., 1992), agrin (Gee et al., 1994; Campanelli et al., 1994), perlecan (Peng et al., 1998; Kanagawa et al., 2005), and neurexin (Sugita et al., 2001). In skeletal muscle, the laminin-α-DG linkage is thought to be critical for plasma membrane stability (recently reviewed in Kanagawa and Toda 2006). In MEB muscle, the α-DG core protein is preserved but hypo-glycosylated, and α-DG prepared from the muscle fails to bind laminin *in vitro* (Michele et al., 2002). Therefore, it is proposed that the disruption of the α-DG-laminin linkage is the main pathomechanism of dystrophic changes seen in MEB muscle.

To further elucidate the molecular pathogenesis of MEB disease, we generated *POMGnT1*-knockout mice using a gene targeting technique, and examined the mutant skeletal muscle. During our experiments, Liu et al. reported the generation of POMGnT1-deficient mice (Liu et al., 2006). The report showed severe muscle pathology, but the mechanism by which POMGnT1 deficiency causes muscle phenotype was not clearly shown. In this report, we report that POMGnT1-deficient mice show remarkably minimal signs of muscle degeneration and regeneration, but also show small muscle mass, reduced numbers of muscle fibers, and impaired muscle regeneration. POMGnT1-deficient myoblasts proliferate poorly *in vitro*. The proliferation was not improved by retrovirus vector-mediated *POMGnT1* expression in *POMGnT1*$^{-/-}$ myoblasts, suggesting that α-DG–laminin interaction *in vivo* is important for maintenance of the proliferative activity of satellite cells.

2. Results

2.1. *Inactivation of the POMGnT1 gene in mice*

We mutated the *POMGnT1* gene by replacing exon 18 with a neomycin-resistance gene in mouse ES cells (depicted in Fig. 1). Two ES clones successfully entered the germline. Although there was no evidence of embryonic lethality, more than 60% of the homozygotes died within 3 weeks of birth. Survivors were smaller than their wild-type littermates (Fig. 3A) throughout life, but most of them had a normal life span. We confirmed that the *POMGnT1*$^{-/-}$ mice completely lacked the POMGnT1 enzyme activity (Fig. 2A). A monoclonal antibody, VIA4-1, that reacts with the suger moiety of α-DG gave no signal in either *POMGnT1*$^{-/-}$ brain (Fig. 2B) or muscle (data not shown). A polyclonal antibody against α-DG core protein revealed that the *POMGnT1*$^{-/-}$ brain expresses approximately 80 kDa α-DG protein, which is much smaller than that seen in the wild-type brain (ca. 110 kDa) (Fig. 2C). We next examined whether α-DG in *POMGnT1*$^{-/-}$ brain binds laminin. Wheat germ agglutinin (WGA)-enriched brain protein from control and *POMGnT1*$^{-/-}$ mice was separated on SDS–PAGE gels, blotted onto a PVDF membrane, incubated with EHS laminin, and then bound laminin was detected by an anti-laminin antibody. α-DG in *POMGnT1*$^{-/-}$ brain failed to bind to laminin (Fig. 2D).

2.2. *POMGnT1*$^{-/-}$ *muscle shows very mild dystrophic changes*

Immunohistochemistry of cross-sections of tibialis anterior (TA) muscles showed that dystrophin and other members of the DGC complex were normally expressed at the sarcolemma of *POMGnT1*$^{-/-}$ muscle (Fig. 3 and Table 1). Laminin α2 chain was detected around POMGnT1$^{-/-}$ muscle fibers. On H.E.-stained cross-sections, surprisingly, the POMGnT1$^{-/-}$ muscle showed almost normal morphology. Central nucleation of myofibers indicates regeneration events in the past. In the TA muscles of 4-week-old wild-type mice, 0.25% of myofibers were centrally nucleated. In POMGnT1$^{-/-}$ mice, 0.28% of the myofibers had central nuclei. In contrast, ca. 40–50% of myofibers of age-matched mdx mice were centrally nucleated. Even at 24 months of age, the percentage of centrally nucleated myofibers was lower (3.6%) in POMGnT1$^{-/-}$ TA muscle, compared with age-matched wild-type TA muscle (9.0%). POMGnT1$^{-/-}$ TA muscle also lacked other signs of degeneration and regeneration. Electrophoresis of muscle extracts on glycerol SDS–PAGE gels showed no difference in MyHC isoform composition of quadriceps and gastrocnemius muscles between POMGnT1$^{-/-}$ and wild-type littermates (data not shown). In both wild-type and POMGnT1$^{-/-}$ muscle, the muscle basal lamina was normally formed (Supplementary Fig. 1). Electron microscopy also showed that the sarcomere structures are almost normal in POMGnT1$^{-/-}$ mice. We next examined the serum creatine kinase (CK) levels, an index of on-going muscle damage, in wild-type, POMGnT1$^{-/-}$, and age-matched mdx mice (Fig. 5). The serum CK levels of 5- to 20-week-old POMGnT1$^{-/-}$ mice were slightly higher (av. 586 U/L, $n = 10$) ($p < 0.05$) than those of wild-type littermates (less than 100 U/L, $n = 4$), but were much lower than those of mdx mice (more than 5000 U/L, $n = 3$, $p < 0.01$). The serum CK levels of 2-year-old POMGnT1$^{-/-}$ mice were still low (less than 300 U/L, $n = 4$).

2.3. *Repetitive muscle injury causes more fibrosis and fatty infiltration in POMGnT1*$^{-/-}$ *than in WT TA muscle*

Dystroglycans expressed on the cell membrane of satellite cells are proposed to play an important role in muscle regeneration (Cohn et al., 2002). In addition, the average size of *POMGnT1*$^{-/-}$ myofibers was smaller than those of wild-type myofibers (Fig. 4). Moreover, the number of myofibers is reduced in *POMGnT1*$^{-/-}$ skeletal muscle of neonatal and adult POMGnT1 mice, suggesting proliferation defect of *POMGnT1*$^{-/-}$ myoblasts (Fig. 4). To test the hypothesis, we damaged *POMGnT1*$^{-/-}$ TA muscle by cardiotoxin (CTX) and examined their regeneration. After single cardiotoxin injection, *POMGnT1*$^{-/-}$ muscle regenerated well like wild-type (data not shown). Next, we injected CTX into TA muscles of *POMGnT1*$^{-/-}$ and heterozygous littermates three times at intervals of 2 weeks, or 1 week interval, and examined the muscle. We summarized the results in Fig. 6. *POMGnT1*$^{-/-}$ muscle showed more fibrosis and

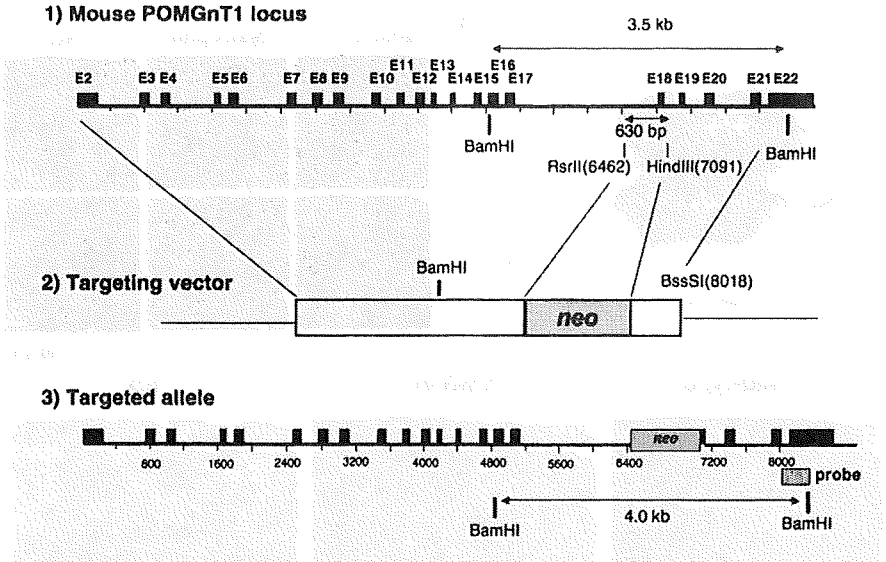

Fig. 1 – Targeted disruption of the mouse *POMGnT1* gene in embryonic stem (ES) cells. The successfully targeted allele lacks a 630 bp-genome fragment containing exon 18, and instead has a *neo* resistance gene. Recombination in ES cells was confirmed by Southern blotting with the probe shown by a shaded box. The nucleic acid numbers are from AB053221 in GenBank.

fatty infiltration, which is a sign of inefficient muscle regeneration, than *POMGnT1*$^{+/-}$ muscle. Together with reduced numbers of myofibers in muscle, the results suggest that the function of satellite cells in *POMGnT1*$^{-/-}$ skeletal muscle is impaired.

2.4. *Defective proliferative activity of POMGnT1*$^{-/-}$ *myoblasts*

We next tested activation and proliferation of satellite cells on living myofibers isolated from wild-type and *POMGnT1*$^{-/-}$

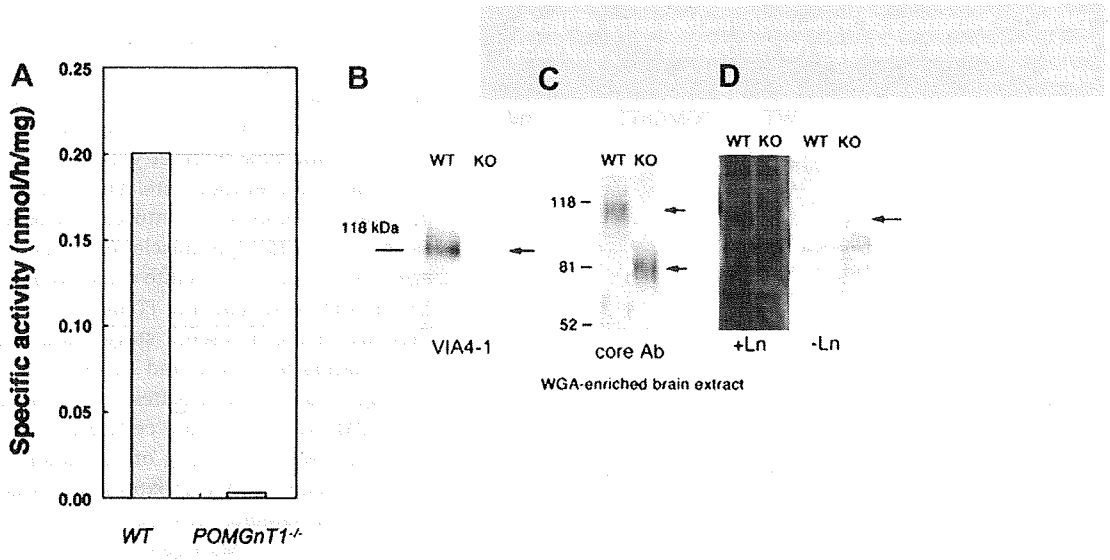

Fig. 2 – *POMGnT1*$^{-/-}$ mice show undetectable POMGnT1 enzyme activity and aberrant glycosylation of α-dystroglycan (α-DG) in *POMGnT1*$^{-/-}$ mice. (A) The amount of POMGnT1 activity is based on the amount of [^{3}H]GlcNAc transferred from UDP-GlcNAc to mannosyl peptide. The reaction product was purified by reverse-phased HPLC, and the radioactivity was measured. (B) Wheat germ agglutinin (WGA) agarose-enriched brain extracts from wild-type (WT) or *POMGnT1*$^{-/-}$ (KO) mice were resolved on a 7.5% SDS–PAGE gel, transferred to a PVDF membrane, and probed with anti-α-DG antibody, VIA4-1, which recognizes glycosylated α-DG. (C) The blot was incubated with polyclonal antibodies specific for α-DG core protein. The antibody detected ~110 kDa bands in wild-type brain extract, and 80 kDa bands in the brain extract of *POMGnT1*$^{-/-}$ mice. (D) Laminin overlay assay showing that α-DG in *POMGnT1*$^{-/-}$ brain does not bind laminin *in vitro*. +Ln, laminin was incubated with the blotted membrane. -LN, without laminin.

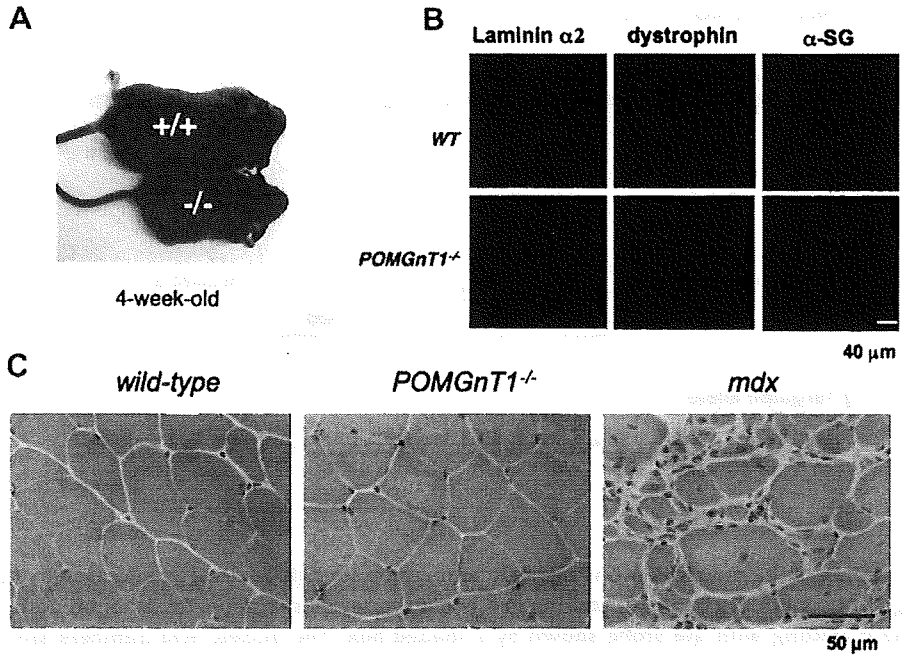

Fig. 3 – Remarkably mild dystrophic phenotypes of *POMGnT1*$^{-/-}$ muscle. (A) A photo of representative 4-week-old wild-type (+/+) and *POMGnT1*$^{-/-}$ (−/−) mice. *POMGnT1*$^{-/-}$ mice are smaller than wild-type littermates. (B) Immunohistochemistry of wild-type (+/+) and POMGnT1-knockout (−/−). Laminin α2 chain, dystrophin, and α-sarcoglycan are expressed normally on the sarcolemma of *POMGnT1*$^{-/-}$ muscle. (C) Representative H.E. staining of cross-sections of the TA muscles from *POMGnT1*$^{-/-}$, wild-type, and age-matched dystrophin-deficient *mdx* mice. *POMGnT1*$^{-/-}$ muscle shows minimal signs of degeneration and regeneration.

Table 1 – Summary of immunohistochemistry of hind-limb muscles of wild-type (WT) POMGnT1$^{-/-}$, and mdx mice.

	WT	*POMGnT1*$^{-/-}$	*mdx*
Laminin α2 chain	+	+	+
Dystrophin	+	+	−
α-Dystroglycan (VIA4-1)	+	−	±
Dystroglycan (core protein)	+	+	±
β-Dystropglycan	+	+	±
α-Sarcoglycan	+	+	±
α-Syntrophin	+	+	±
nNOS	+	+	±
Aquaporin 4	+	+	±
Integrin α7	+	+	++
Integrin β1	+	+	++

+, expressed; −, absent; ±, down-regulated; ++, up-regulated.

mice (Fig. 7). Three days after plating of single myofibers on Matrigel-coated 24-well plates in growth medium, the numbers of detached satellite cells (activated and proliferating satellite cells) were counted. In both extensor digitorum longus (EDL) (fast twitch muscle) and soleus (slow twitch muscle) muscles, the numbers of activated satellite cells and proliferating satellite cells (myoblasts) around the parental myofiber were more numerous in wild-type than in *POMGnT1*$^{-/-}$ (Fig. 7). Furthermore, wild-type satellite cells migrate a little faster than *POMGnT1*$^{-/-}$ satellite cells on transwells (data not shown), although the difference was little. Therefore, our results suggest that *POMGnT1*$^{-/-}$ satellite cells are activated more slowly or proliferate more slowly than wild-type. We next isolated satellite cells from hind limb muscles of wild-type and *POMGnT1*$^{-/-}$ mice by a monoclonal antibody, SM/C-2.6, and flow cytometry (Fukada et al., 2007), and examined their proliferation rate. The total yield of satellite cells per gram of *POMGnT1*$^{-/-}$ muscle tissue was nearly the same as those of wild-type muscle (data not shown). The percentage of Ki67-positive satellite cells (cycling cells) was less than 1% in both wild-type and *POMGnT1*$^{-/-}$ mice, indicating that they are in the quiescent stage (data not shown). However, after plating wild-type and *POMGnT1*$^{-/-}$ satellite cells onto Matrigel-coated 6-well plates at the same density, we found that *POMGnT1*$^{-/-}$ satellite cells grew poorly in growth medium (Fig. 7B). The timing of activation (i.e. enlargement of the cytoplasm and MyoD expression) was the same with that of wild-type satellite cells (data not shown). Next, we cultured satellite cells on Matrigel-coated 24-well-plates in growth medium, and the cells growth was evaluated by MTT assay 1, 2, 3, 4, 5, 6, and 7 days after plating (Fig. 8). The assay revealed that wild-type myoblasts proliferated more rapidly than *POMGnT1*$^{-/-}$ myoblasts *in vitro*. *POMGnT1*$^{-/-}$ myoblasts fused normally to form multinucleated myotubes in differentiation conditions like the wild-type (data not shown), and there was no significant difference in the fusion index between wild-type (45%) and *POMGnT1*$^{-/-}$ myoblasts (40%) ($p > 0.05$).

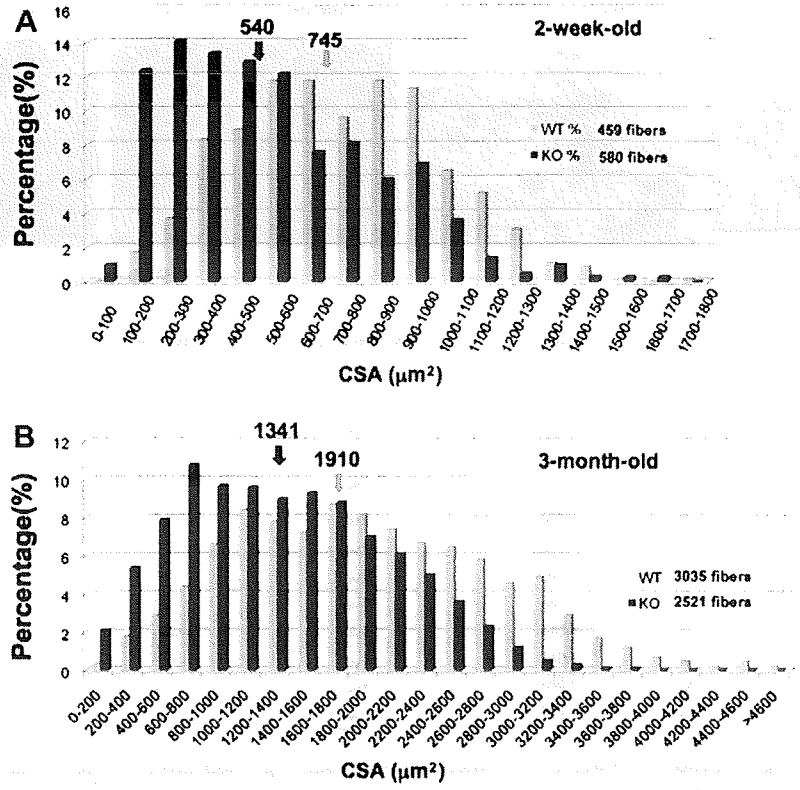

Fig. 4 – Cross-sectional area (CSA) of myofibers of *POMGnT1*$^{-/-}$ and wild-type mice. (A) A representative frequency graph of CSA of rectus femoris muscles from 2-week-old *POMGnT1*$^{-/-}$ (blue) and wild-type (light blue) littermates. The cross-sections were stained with anti-laminin α2 chain antibody. CSA of 459 *POMGnT1*$^{-/-}$ fibers and 580 wild-type fibers were measured and plotted. X-axis indicates CSA (μm²), and Y-axis indicates percentages. Arrows indicate the averages. The total number of myofibers was also reduced in *POMGnT1*$^{-/-}$ mice (4169 vs. 3510). (B) The CSA of myofibers in TA muscles from 3-month-old *POMGnT1*$^{-/-}$ (blue) and wild-type (light blue) male mice was plotted as in (A)). In (B), almost all myofibers were measured (3035 fibers in wild-type TA and 2521 fibers in *POMGnT1*$^{-/-}$ TA).

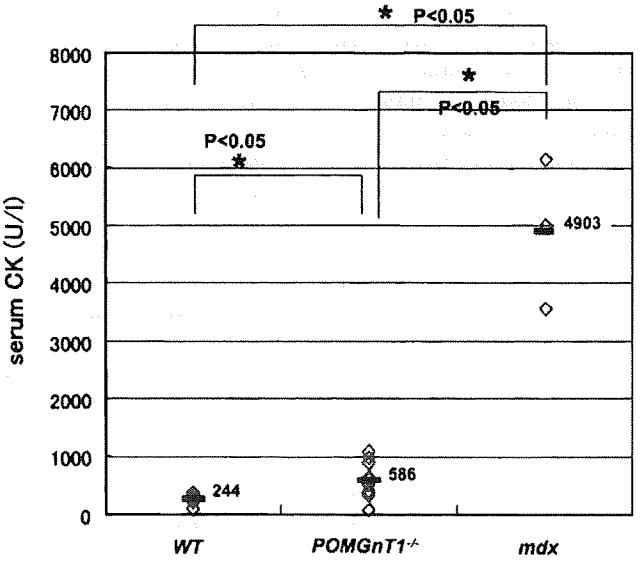

Fig. 5 – Serum CK levels of *POMGnT1*$^{-/-}$, wild-type, and *mdx* mice. Serum CK levels of 7–20 weeks old *POMGnT1*$^{-/-}$ mice (5 males and 5 females), wild-type littermates (3 males and 1 female), and three male *mdx* mice were measured and plotted on the graph with average. *$p < 0.05$.

Next, we examined whether restoration of the expression of the *POMGnT1* gene in mutant myoblasts improved their proliferation. To this end, we prepared a retrovirus vector, (pMX-POMGnT1-IRES-GFP) expressing human *POMGnT1* and GFP. The recombinant retrovirus successfully restored O-mannosyl glycosylation of α-DG (Fig. 7A), but the proliferation rate was not changed (Fig. 8B).

2.5. *Cell growth signaling in POMGnT1*$^{-/-}$ *myoblasts*

It was previously reported that enhanced expression of α7β1 integrin ameliorates the development of muscular dystrophy and extends longevity in α7BX2-*mdx/utr*($^{-/-}$) transgenic mice (Burkin et al., 2001; Burkin et al., 2005), suggesting that integrin compensates for the function of α-DG in skeletal muscle to some extent. Therefore, we next examined the expression of β1-integrin in wild-type and *POMGnT1*$^{-/-}$ myoblasts (Supplementary Fig. 1). Western blotting, however, showed no difference between the β1-integrin protein levels in wild-type and *POMGnT1*$^{-/-}$ myoblasts (Supplementary Fig. 1A). Furthermore, FACS analysis showed similar levels of β1 integrin expression on the surfaces of myoblasts (Supplementary Fig. 1B). We then examined the activation levels of Akt and GSK-3β, both of which are involved in the

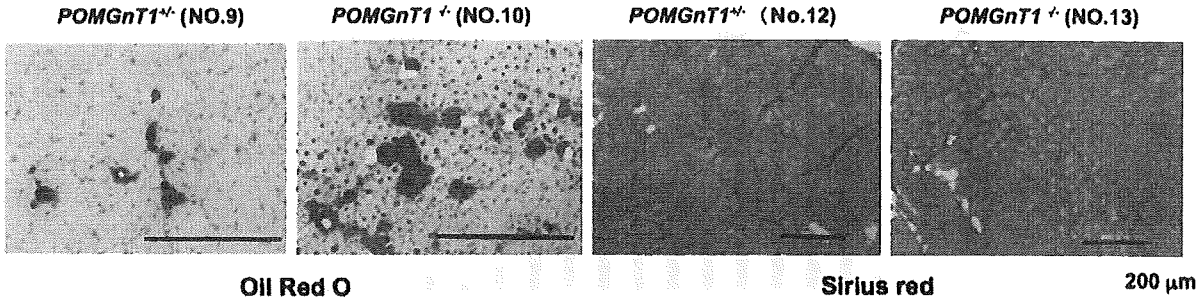

	genotype	sex	age	CTX interval(x3)	Fatty infiltration	Fibrosis
1	+/-	F	3M	2w	-	-
2	+/-	F	3M	2w	-	-
3	+/-	F	3M	2w	- →	- →
4	+/-	F	3M	2w	+	- →
5	-/-	M	3M	2w	+	- →
6	-/-	F	3M	2w	++	- →
7	+/-	F	11M	1w	+	+
8	-/-	F	8.5M	1w	+	++
9	+/-	F	8.5M	1w	+	- →
10	-/-	F	8.5M	1w	+ → ++	+ → ++
11	+/-	M	8.5M	1w	+	+
12	+/-	M	8.5M	1w	++	+
13	-/-	M	8.5M	1w	++	++

Fig. 6 – Impaired muscle regeneration of *POMGnT1*$^{-/-}$ mice. upper panel: representative Oil red O-stained or Sirius red-stained cross-sections of TA muscles of *POMGnT1*$^{-/-}$ (−/−) and *POMGnT1*$^{+/-}$ (+/−) mice after three rounds of degeneration/regeneration evoked by cardiotoxin injection. One week after the last CTX injection, TA muscles were dissected, sectioned by a cryostat, fixed, and stained. lower table: Summary of fatty infiltration and fibrosis in regenerated muscles. CTX was injected into TA muscles three times with 2 weeks interval (2w) or 1 week interval (1w). The age at the first injection was shown. (−), well regenerated with minimal changes. (−→+), sporadic fatty regeneration or slight fibrosis between fibers. (+), mild fatty infiltration or mild fibrosis. (++), dense fatty infiltration or extensive fibrosis. F, female; M, male.

regulation of cell survival and proliferation. The levels of phosphorylation of these two kinases in *POMGnT1*$^{-/-}$ myoblasts were similar with those in wild-type myoblasts (Supplementary Fig. 1C). Consistent with these observations, TUNEL assay indicated that apoptosis is rare both in *POMGnT1*$^{-/-}$ and wild-type muscles (data not shown).

3. Discussion

In this study, we showed that in spite of mild muscle degeneration, the *POMGnT1*$^{-/-}$ satellite cells have much lower proliferative activity than wild-type satellite cells. The defect was not recovered by restoration of normal glycosylation of α-DG in mutant satellite cells. Together with the reduced sizes and the reduced numbers of myofibers of neonatal and adult *POMGnT1*$^{-/-}$ mice, these observations suggest that deficiency of POMGnT1 enzymatic activity impairs the functions of satellite cells.

3.1. *Two mouse models of muscle–eye–brain (MEB) disease*

Our *POMGnT1*$^{-/-}$ mice are the second mouse model of MEB disease. The first one was generated by gene trapping with a retroviral vector inserted into the second exon of the mouse *POMGnT1* locus (Liu et al., 2006). As described in the literature, the phenotype is similar to ours with some differences. Our model shows much milder muscle phenotypes than the previously reported model, but also shows much a lower survival rate in the postnatal stage than the first model does. This would be due to more severe developmental abnormalities of the central nervous system of our mouse model, including disruption of the glia limitans, abnormal migration of neurons, and reactive gliosis in the cerebral cortex (manuscript in preparation), although these are also observed in the first model (Yang et al., 2007; Hu et al., 2007).

Mutation of the *POMGnT1* gene is the cause of muscle–eye–brain disease (MEB) (Yoshida et al., 2001), which is characterized by severe congenital muscular dystrophy (Voit and Tome, 2004). Although glycosylation of α-DG was completely perturbed in our model, the *POMGnT1*$^{-/-}$ muscle showed only marginal pathological changes. Furthermore, *POMGnT1*$^{-/-}$ muscle showed normally formed muscle basal lamina on EM. These observations are in sharp contrast to the condition in humans. One possibility is that in the mouse, molecules other than α-DG are involved in the linkage of the sarcolemma with the extracellular matrix proteins, stabilizing the plasma membrane. As a candidate molecule, we examined β1-integrin expression in *POMGnT1*$^{-/-}$ muscle, but found that the level was not up-regulated. Therefore, the mechanism that explains this discrepancy remains to be clarified in a future study.

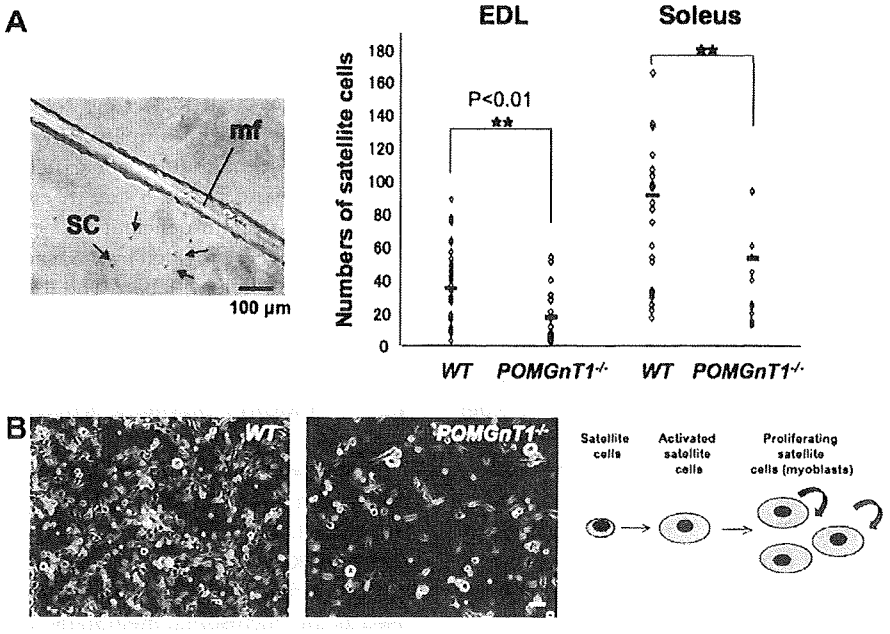

Fig. 7 – Activation and proliferation of satellite cells from WT and *POMGnT1*$^{-/-}$ mice. (A) Isolated myofibers were plated on Matrigel-coated 24 well-plates at one myofiber per well. Three days later, activated satellite cells (SC, arrows) around the parental fiber (mf) were counted and plotted. Small horizontal bars indicate the average number of activated/proliferating satellite cells originating from a myofiber from three independent experiments. Student's *t*-test. $^{**}p < 0.01$ (wild-type vs. *POMGnT1*$^{-/-}$ mice). (B) Satellite cells from WT and *POMGnT1*$^{-/-}$ mice 7 days after plating onto Matrigel-coated 24-well-plates at 2.5×10^3 cells/well. Scale bar, 100 μm.

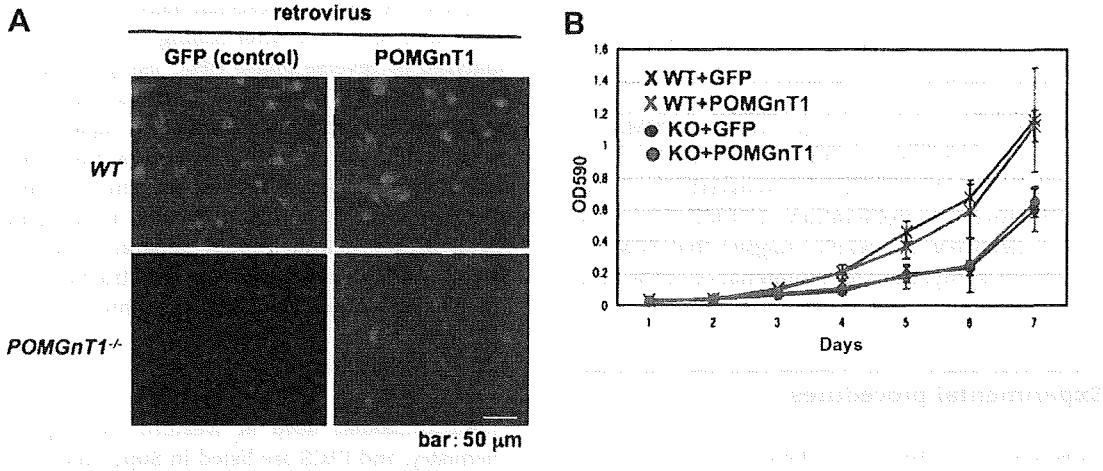

Fig. 8 – Restoration of POMGnT1 expression in *POMGnT1*$^{-/-}$ myoblasts does not improve proliferation of cells. (A) Wild-type (WT) and *POMGnT1*$^{-/-}$ myoblasts were transduced with a retrovirus expressing both POMGnT1 and GFP (POMGnT1) or only GFP (GFP, control), and the FACS-purified transduced cells were stained with anti-glycosylated α-DG monoclonal antibody (VIA4-1; red) and DAPI (Nucleus, blue). Note that the glycosylation of α-DG in *POMGnT1*$^{-/-}$ myoblasts was completely recovered by a retrovirus vector expressing POMGnT1. (B) MTT assay of wild-type (WT) and *POMGnT1*$^{-/-}$ myoblasts after infection with retrovirus vectors. Impaired proliferation of *POMGnT1*$^{-/-}$ myoblasts was not recovered by retrovirus-mediated expression of *POMGnT1*. Representative data of three independent experiments are shown.

3.2. *Null mutation in POMGnT1 reduces proliferative activity of muscle satellite cells*

POMGnT1$^{-/-}$ myoblasts proliferate poorly *in vitro*. This observation suggested that the proliferation of myoblasts is stimulated by growth signals *via* laminin-α-DG interaction. However, retrovirus vector-mediated gene transfer of the *POMGnT1* gene, which successfully restored O-mannosyl glycosylation of α-DG, did not restore the proliferation activity of the *POMGnT1*$^{-/-}$ myoblasts. DMD myoblasts proliferate poorly and quickly reach senescence. The impaired proliferation activity has been ascribed to repeated activation of

satellite cells due to repetitive cycles of muscle degeneration and regeneration (Blau et al., 1983). In contrast, POMGnT1$^{-/-}$ muscle lacks signs of active regeneration. Therefore, the reduced proliferation activity of POMGnT1$^{-/-}$ mouse myoblasts is not likely due to excessive cell division of satellite cells. Rather, it is likely that α-DG-laminin interaction in the niche, i.e. beneath the basal lamina of skeletal muscle myofibers, is important for maintenance of proliferative activity of satellite cells. However, the possibility that POMGnT1-deficiency causes aberrant glycosylation of molecules other than α-DG should be also tested.

Our results also suggested that the lack of α-DG-laminin interaction resulted in reduced numbers of muscle fibers (hypoplasia). Importantly, we found that myofibers of older POMGnT1$^{-/-}$ mice tend to be hypertrophied (Supplementary Fig. 2). POMGnT1$^{-/-}$ muscle might compensate the muscle power by hypertrophy of the myofibers. This is consistent with our observation that POMGnT1$^{-/-}$ muscle increases its mass in an overload model (unpublished data). Importantly, recent studies suggest that this process is satellite cell-independent (Sandri M., 2008).

Recently, Liu et al. showed that over-expression of integrin α7β1 in C2C12 myoblasts promoted proliferation of the cells (Liu et al., 2008). Importantly, however, we did not observe up-regulation of integrin α7β1 expression in POMGnT1$^{-/-}$ satellite cells. These observations suggest that dystroglycans and integrins have distinct roles in the regulation of muscle satellite cells.

In summary, we generated POMGnT1-null mice. The mice showed low serum creatine kinase levels and minimal signs of muscle degeneration and regeneration. Nonetheless, POMGnT1$^{-/-}$ muscle showed the reduction in the size and the number of myofibers. Furthermore, repeated injection of cardiotoxin showed impaired muscle regeneration in POMGnT1$^{-/-}$ mice. POMGnT1$^{-/-}$ myoblasts proliferated poorly *in vitro*. Over-expression of protein restored glycosylation of α-DG, but did not improve the proliferation of POMGnT1$^{-/-}$ myoblasts at all. Collectively, our results suggest that POMGnT1 enzymatic activity is important for maintenance of the proliferative activity of satellite cells *in vivo*.

4. Experimental procedures

4.1. Generation of POMGnT1$^{-/-}$ mice

The targeting strategy in ES cells is depicted in Fig. 1. Genomic DNA (8.6 kb) covering almost the entire POMGnT1 gene was isolated from 129/SvJ mice by using two specific primers: m1F2 primer, 5′-gat tcc tga agt cat gga ctg gc-3′ and m1B5, 5′-tct aaa ggt ctc tgt gtg agt ctg tca g-3′. The PCR product was then cloned into a TOPO TA cloning vector (Invitrogen, Carlsbad, CA) and sequenced (AB053221). To construct the targeting vector, a 630-bp RsrII-Hind III fragment, containing exon18 was replaced with a *neo* expression cassette (Stratagene) (Fig. 1). Electroporation and screening of ES cells (129Svev origin) were performed by Ingenious Targeting Laboratory, Inc. (Stony Brook, NY). Homologous recombination in ES cells was confirmed by Southern blotting. Two independent positive ES clones were injected into C57BL/6 blastocysts, which gave rise to offspring carrying the mutated allele. Genotyping of the mice was done by PCR. One primer set is designed to amplify exon 18: F2, 5′-cag cag ttt cct tcc ttc taa ccc-3′ and B4, 5′-att tgg tct ggt ccc ttg gct c-3′ (278 bp). *Neo* primers were used to amplify the *neo* resistance gene, and thereby detect the mutant allele: neo-F, 5′-agg cta ttc ggc tat gac tgg g-3′, and neo-R, 5′-tac ttt ctc ggc agg agc aag gtg-3′ (288 bp). Dystrophin-deficient *mdx* mice of C57BL/6 genetic background were provided by T. Sasaoka at the National Institute for Basic Biology, Japan. The Experimental Animal Care and Use Committee of the National Institute of Neuroscience approved all experimental protocols.

4.2. POMGnT1 enzymatic activity

Brains were obtained from 8-week-old mice and homogenized with nine volumes (weight/volume) of 10 mM Tris–HCl, pH 7.4, 1 mM EDTA, and 250 mM sucrose. After centrifugation at 900*g* for 10 min, the supernatant was subjected to ultracentrifugation at 100,000*g* for 1 h. The precipitates were used as the microsomal membrane fraction. The protein concentration was determined by BCA assay (Pierce, Rockford, IL). The enzymatic activity assay measured the amount of [^{3}H]GlcNAc transferred to a mannosyl peptide (Akasaka-Manya et al., 2004). Briefly, a reaction mixture containing 140 mM Mes buffer (pH 7.0), 1 mM UDP-[^{3}H]GlcNAc (80,000 dpm/nmol, PerkinElmer, Inc., Wellesley, MA), 2 mM mannosyl peptide (Ac-Ala-Ala-Pro-Thr-(Man)-Pro-Val-Ala-Ala-Pro-NH_2), 10 mM $MnCl_2$, 2% Triton X-100, 5 mM AMP, 200 mM GlcNAc, 10% glycerol, and 100 μg of microsomal membrane fraction was incubated at 37 °C for 1 h. After boiling for 3 min, the mixture was analyzed by reverse phase HPLC using a Wakopak 5C18-200 column (4.6 × 250 mm, Wako Pure Chemical Industries, Osaka, Japan). The gradient solvents were aqueous 0.1% trifluoroacetic acid (solvent A) and acetonitrile containing 0.1% trifluoroacetic acid (solvent B). The mobile phase consisted of 100% A for 10 min and then a linear gradient to 75% A:25% B over 25 min. Peptide separation was monitored at 214 nm, and the radioactivity of each fraction (1 ml) was measured using a liquid scintillation counter.

4.3. Antibodies

All antibodies used in Western blotting, immunohistochemistry, and FACS are listed in Supplementary Table 1.

4.4. Histology and immunohistochemical analysis

Muscle cryosections (6–10 μm) were stained with hematoxylin and eosin (H&E), or treated with 0.1% Triton X-100, blocked with 5% goat serum/1% BSA in PBS, then incubated with primary antibodies (Supplementary Table 1) at 4 °C overnight. After washing with PBS, specimens were incubated with a secondary antibody labeled with Alexa Fluor 488 or Alexa Fluor 568 (1:200–400 dilution; Molecular Probes) at RT for 1 h, counterstained with TOTO-3 (1:5000; Molecular Probes), and then mounted in Vectashield (Vector). The images were recorded using a confocal laser scanning microscope system TCSSP™ (Leica). For fiber size measurement, cross-sections of muscle were stained with anti-laminin α2

antibody and recorded and quantified by a digital microscope, BIOREVO (http://www.biorevo.jp; KEYENCE, Osaka, Japan).

4.5. Western blotting

Western blotting was performed as previously described (Hosaka et al., 2002). In brief, 20 μg of muscle proteins were separated on 7.5% SDS–PAGE gels and transferred to a PVDF membrane (Millipore, Bedford, MA). After incubation with primary antibodies (Supplementary Table 1), the membranes were incubated in HRP-labeled secondary antibodies (1:5000 dilution) (Amersham Biosciences, UK). The signals were detected by using an ECL plus Western Blotting Detection System (GE Healthcare, Buckinghamshire, UK).

4.6. Laminin blot overlay assay

An overlay assay was performed as described by Moore et al. (2002). In brief, WGA-enriched homogenates were prepared from wild-type and *POMGnT1*$^{-/-}$ brains, separated on SDS–PAGE gels, blotted onto a PDVF membrane, and incubated with mouse EHS laminin (Trevigen, Gaithersburg, MD, USA). Bound laminin was probed with anti-laminin antibody (Sigma, St. Louis, MO) and ECL system (GE Healthcare, Buckinghamshire, UK).

4.7. Single fiber preparation and culture

Single fibers were prepared from extensor digitorum longus (EDL) and soleus muscles of wild-type and *POMGnT1*$^{-/-}$ mice as described by Rosenblatt et al. (1995). Each fiber was plated onto Matrigel (BD Biosciences, Bedford, MA)-coated 24-well plates and cultured in growth medium for 3 days. Then, the number of cells around the parental fiber was counted.

4.8. Isolation of satellite cells, proliferation assay, and fusion index

Satellite cells were prepared from wild-type and *POMGnT1*$^{-/-}$ mice by FACS as previously described (Fukada et al., 2007). Sorted cells were plated on Matrigel-coated 24-well-plates at a density of 1×10^4 cells/well in a growth medium, DMEM (High glucose; Wako, Osaka), supplemented with 20% fetal bovine serum (Equitech-bio, Inc., Kerville, TX), human recombinant bFGF (2.5 ng/ml) (Invitrogen), recombinant mouse HGF (25 ng/ml) (R&D Systems, Minneapolis, MN), and heparin (5 μg/ml) (Sigma). For the MTT assay, 100 μl of 0.5% MTT (3-(4,5-dimethylthiazol-2-yl)-2,5-diphenyltetrazolium bromide) (Dojindo, Kumamoto, Japan) was added to the culture at each time point, and after 4 h incubation, the cells were collected in 1 ml of acid isopropanol solution. OD_{590} was measured and plotted. After reaching 70% confluency, the cells were induced to differentiate into myotubes by low-serum medium (5% horse serum/DMEM), and 18 h later, the cells were fixed, stained with anti-sarcomeric α-actinin antibody and DAPI (nuclei). Fusion index was calculated as (the numbers of nuclei in the myotubes/total nuclei) × 100%.

4.9. Production of retrovirus vectors

pMXs-IG (Kitamura et al., 2003) was kindly provided by T.Kitamura at Tokyo University. Human POMGnT1 cDNA, which has an Xpress epitope and a His-tag at the N-terminal (Akasaka-Manya et al., 2004), was cloned into the multi-cloning site upstream of IRES-GFP of the vector. Vector particles were produced by transfection of the vector plasmid into PLAT-E packaging cells (Kitamura et al., 2003). Proliferating satellite cells (myoblasts) were incubated with the viral vectors overnight and 4 days later, successfully transduced GFP-positive cells were collected by FACS, and the proliferation rate was evaluated by MTT assay.

4.10. Electron microscopy

Mice were perfused transcardially with a solution of 2% paraformaldehyde and 2.5% glutaraldehyde in PBS under deep pentobarbital anesthesia. The anterior tibial muscles were excised, embedded in 3% agarose, and sections (70 μm in thickness) were prepared on a Vibratome. Sections were fixed in OsO_4, ehydrated, and embedded in Cartepoxy resin. Ultrathin sections were prepared, stained with lead citrate and uranyl acetate, and observed under a Hitachi H-7000 transmission electron microscope.

4.11. Measurement of serum creatine kinase (CK)

Blood samples were obtained from the tail vein or directly from the heart at sacrifice. Serum CK level was measured by colorimetric assay using an FDC3500 clinical biochemistry autoanalyzer (FujiFilm Medical Co., Tokyo, Japan).

4.12. Cardiotoxin (CTX) injection

To induce muscle regeneration, CTX (10 μmol/L in saline; Sigma, St. Louis, MO) was injected into the tibialis anterior (TA) muscles three times at indicated intervals. The muscle cross-sections were stained with Oil red O (Muto Pure Chemicals Co., Ltd., Tokyo, Japan) to detect lipid droplets, or with Sirius red F3B (Sigma Chemical Co., St. Louis, MO) in saturated picric acid to stain collagen fibers.

Acknowledgments

This work was supported by Health Science Research Grants for Research on the Human Genome and Gene Therapy (H16-genome-003). For research on Phychiatric and Neurological Diseases and Mental Health (H18-kokoro-019; H20-016) from the Japanese Ministry of Health, Labor and Welfare, and Grants-in-Aid for Scientific Research (18590392) from the Japanese Ministry of Education, Culture, Sports, Science and Technology.

Appendix A. Supplementary data

Supplementary data associated with this article can be found, in the online version, at doi:10.1016/j.mod.2008.12.001.

REFERENCES

Akasaka-Manya, K., Manya, H., Kobayashi, K., Toda, T., Endo, T., 2004. Structure-function analysis of human protein O-linked mannose beta1,2-N-acetylglucosaminyltransferase 1, POMGnT1. Biochem. Biophys. Res. Commun. 320, 39–44.

Blau, H.M., Webster, C., Pavlath, G.K., 1983. Defective myoblasts identified in Duchenne muscular dystrophy. Proc. Natl. Acad. Sci. USA 80, 4856–4860.

Burkin, D.J., Wallace, G.Q., Milner, D.J., Chaney, E.J., Mulligan, J.A., Kaufman, S.J., 2005. Transgenic expression of α7β1 integrin maintains muscle integrity, increases regenerative capacity, promotes hypertrophy, and reduces cardiomyopathy in dystrophic mice. Am. J. Pathol. 166, 253–263.

Burkin, D.J., Wallace, G.Q., Nicol, K.J., Kaufman, D.J., Kaufman, S.J., 2001. Enhanced expression of the alpha 7 beta 1 integrin reduces muscular dystrophy and restores viability in dystrophic mice. J. Cell Biol. 152, 1207–1218.

Campanelli, J.T., Roberds, S.L., Campbell, K.P., Scheller, R.H., 1994. A role for dystrophin-associated glycoproteins and utrophin in agrin-induced AChR clustering. Cell 77, 663–674.

Cohn, R.D., Henry, M.D., Michele, D.E., Barresi, R., Saito, F., Moore, S.A., Flanagan, J.D., Skwarchuk, M.W., Robbins, M.E., Mendell, J.R., Williamson, R.A., Campbell, K.P., 2002. Disruption of DAG1 in differentiated skeletal muscle reveals a role for dystroglycan in muscle regeneration. Cell 110, 639–648.

Endo, T., Toda, T., 2003. Glycosylation in congenital muscular dystrophies. Biol. Pharm. Bull. 26, 1641–1647.

Fukada, S., Uezumi, A., Ikemoto, M., Masuda, S., Segawa, M., Tanimura, N., Yamamoto, H., Miyagoe-Suzuki, Y., Takeda, S., 2007. Molecular signature of quiescent satellite cells in adult skeletal muscle. Stem Cells 25, 2448–2459.

Gee, S.H., Montanaro, F., Lindenbaum, M.H., Carbonetto, S., 1994. Dystroglycan-alpha, a dystrophin-associated glycoprotein, is a functional agrin receptor. Cell 77, 675–686.

Hosaka, Y., Yokota, T., Miyagoe-Suzuki, Y., Yuasa, K., Imamura, M., Matsuda, R., Ikemoto, T., Kameya, S., Takeda, S., 2002. Alpha1-syntrophin-deficient skeletal muscle exhibits hypertrophy and aberrant formation of neuromuscular junctions during regeneration. J. Cell Biol. 158, 1097–1107.

Hu, H., Yang, Y., Eade, A., Xiong, Y., Qi, Y., 2007. Breaches of the pial basement membrane and disappearance of the glia limitans during development underlie the cortical lamination defect in the mouse model of muscle-eye-brain disease. J. Comp. Neurol. 502, 168–183.

Ibraghimov-Beskrovnaya, O., Ervasti, J.M., Leveille, C.J., Slaughter, C.A., Sernett, S.W., Campbell, K.P., 1992. Primary structure of dystrophin-associated glycoproteins linking dystrophin to the extracellular matrix. Nature 355, 696–702.

Kanagawa, M., Michele, D.E., Satz, J.S., Barresi, R., Kusano, H., Sasaki, T., Timpl, R., Henry, M.D., Campbell, K.P., 2005. Disruption of perlecan binding and matrix assembly by post-translational or genetic disruption of dystroglycan function. FEBS Lett. 579, 4792–4796.

Kanagawa, M., Toda, T., 2006. The genetic and molecular basis of muscular dystrophy: roles of cell–matrix linkage in the pathogenesis. J. Hum. Genet. 51, 915–926.

Kitamura, T., Koshino, Y., Shibata, F., Oki, T., Nakajima, H., Nosaka, T., Kumagai, H., 2003. Retrovirus-mediated gene transfer and expression cloning: powerful tools in functional genomics. Exp. Hematol. 31, 1007–1014.

Liu, J., Ball, S.L., Yang, Y., Mei, P., Zhang, L., Shi, H., Kaminski, H.J., Lemmon, V.P., Hu, H., 2006. A genetic model for muscle–eye–brain disease in mice lacking protein O-mannose 1,2-N-acetylglucosaminyltransferase (POMGnT1). Mech. Dev. 123, 228–240.

Liu, J., Burkin, D.J., Kaufman, S.J., 2008. Increasing alpha 7 beta 1-integrin promotes muscle cell proliferation, adhesion, and resistance to apoptosis without changing gene expression. Am. J. Physiol. Cell Physiol. 294, C627–C640.

Michele, D.E., Barresi, R., Kanagawa, M., Saito, F., Cohn, R.D., Satz, J.S., Dollar, J., Nishino, I., Kelley, R.I., Somer, H., Straub, V., Mathews, K.D., Moore, S.A., Campbell, K.P., 2002. Post-translational disruption of dystroglycan–ligand interactions in congenital muscular dystrophies. Nature 418, 417–422.

Moore, S.A., Saito, F., Chen, J., Michele, D.E., Henry, M.D., Messing, A., Cohn, R.D., Ross-Barta, S.E., Westra, S., Williamson, R.A., Hoshi, T., Campbell, K.P., 2002. Deletion of brain dystroglycan recapitulates aspects of congenital muscular dystrophy. Nature 418, 422–425.

Peng, H.B., Ali, A.A., Daggett, D.F., Rauvala, H., Hassell, J.R., Smalheiser, N.R., 1998. The relationship between perlecan and dystroglycan and its implication in the formation of the neuromuscular junction. Cell Adhes. Commun. 5, 475–89.

Rosenblatt, J.D., Lunt, A.I., Parry, D.J., Partridge, T.A., 1995. Culturing satellite cells from living single muscle fiber explants. In Vitro Cell Dev. Biol. Anim. 31, 773–779.

Sandri M., 2008. Signaling in muscle atrophy and hypertrophy. Physiology (Bethesda) 23, 160–170.

Sugita, S., Saito, F., Tang, J., Satz, J., Campbell, K., Südhof, T.C., 2001. A stoichiometric complex of neurexins and dystroglycan in brain. J. Cell Biol. 154, 435–445.

Voit, T., Tome, F.S., 2004. The congenital muscular dystrophies. In: Engel, A.G., Franzini-Armstrong, C. (Eds.), Myology. McGraw-Hill, New York, pp. 1203–1238.

Yang, Y., Zhang, P., Xiong, Y., Li, X., Qi, Y., Hu, H., 2007. Ectopia of meningeal fibroblasts and reactive gliosis in the cerebral cortex of the mouse model of muscle-eye-brain disease. J. Comp. Neurol. 505, 459–477.

Yoshida, A., Kobayashi, K., Manya, H., Taniguchi, K., Kano, H., Mizuno, M., Inazu, T., Mitsuhashi, H., Takahashi, S., Takeuchi, M., Herrmann, R., Straub, V., Talim, B., Voit, T., Topaloglu, H., Toda, T., Endo, T., 2001. Muscular dystrophy and neuronal migration disorder caused by mutations in a glycosyltransferase, POMGnT1. Dev. Cell 1, 717–724.

A Renaissance for Antisense Oligonucleotide Drugs in Neurology

Exon Skipping Breaks New Ground

Toshifumi Yokota, PhD; Shin'ichi Takeda, MD, PhD; Qi-Long Lu, MD, PhD; Terence A. Partridge, PhD; Akinori Nakamura, MD, PhD; Eric P. Hoffman, PhD

Antisense oligonucleotides are short nucleic acid sequences designed for use as small-molecule drugs. They recognize and bind to specific messenger RNA (mRNA) or pre-mRNA sequences to create small double-stranded regions of the target mRNA that alter mRNA splicing patterns or inhibit protein translation. Antisense approaches have been actively pursued as a form of molecular medicine for more than 20 years, but only one has been translated to a marketed drug (intraocular human immunodeficiency virus treatment). Two recent advances foreshadow a change in clinical applications of antisense strategies. First is the development of synthetic DNA analogues that show outstanding stability and sequence specificity yet little or no binding to modulator proteins. Second is the publication of impressive preclinical and clinical data using antisense in an exon-skipping strategy to increase dystrophin production in Duchenne muscular dystrophy. As long-standing barriers are successfully circumvented, attention turns toward scale-up of production, long-term toxicity studies, and the challenges to traditional drug regulatory attitudes presented by tightly targeted sequence-specific drugs.

Arch Neurol. 2009;66(1):32-38

With the advent of recombinant DNA in the 1970s, it was soon realized that bacteria possess a form of regulatory machinery where small RNA transcripts can bind (hybridize) to other target RNAs and inhibit the translation of these targets.[1] These antisense RNAs were subsequently recognized as natural translational regulation mechanisms in plants and higher organisms.[2] More recently, a specialized form of antisense transcript was found to be a cellular defense mechanism against invading messenger RNAs (mRNAs) (viruses), and this has been harnessed as a popular method to "knock down" specific mRNA transcripts in cultured cell models (short interfering RNAs).[3]

Attention soon shifted toward development of antisense molecules as a form of small-molecule drug (antisense oligonucleotide [AO]). The approach was intuitive: one needs simply to chemically synthesize short pieces of DNA of about 20 bases, where a specific complementary sequence is designed to hybridize with a desired target mRNA. Such designer AO drugs should show very high specificity and selectivity for binding only the desired target RNA sequence of nucleotides that is predicted by base pairing. Beginning in the mid-1980s, this approach was put to the test in model systems and was shown to work quite well in shutting down the production of the target (undesired) protein.[4] Isis Pharmaceuticals, Inc, Carlsbad, California, a company focused on clinical applications of AOs, was incorporated in 1989. Additional companies focusing on AO approaches soon followed.

Despite early promise, uses of AOs as small-molecule drugs have been painfully slow to enter the market and standard of care. Indeed, only a single AO drug has been approved by the Food and Drug

Author Affiliations: Research Center for Genetic Medicine, Children's National Medical Center, Washington, DC (Drs Yokota, Partridge, and Hoffman); Department of Molecular Medicine, National Institutes for Neuroscience, Tokyo, Japan (Drs Takeda and Nakamura); and McColl-Lockwood Laboratory for Muscular Dystrophy Research, Neuromuscular/ALS Center, Carolinas Medical Center, Charlotte, North Carolina (Dr Lu).

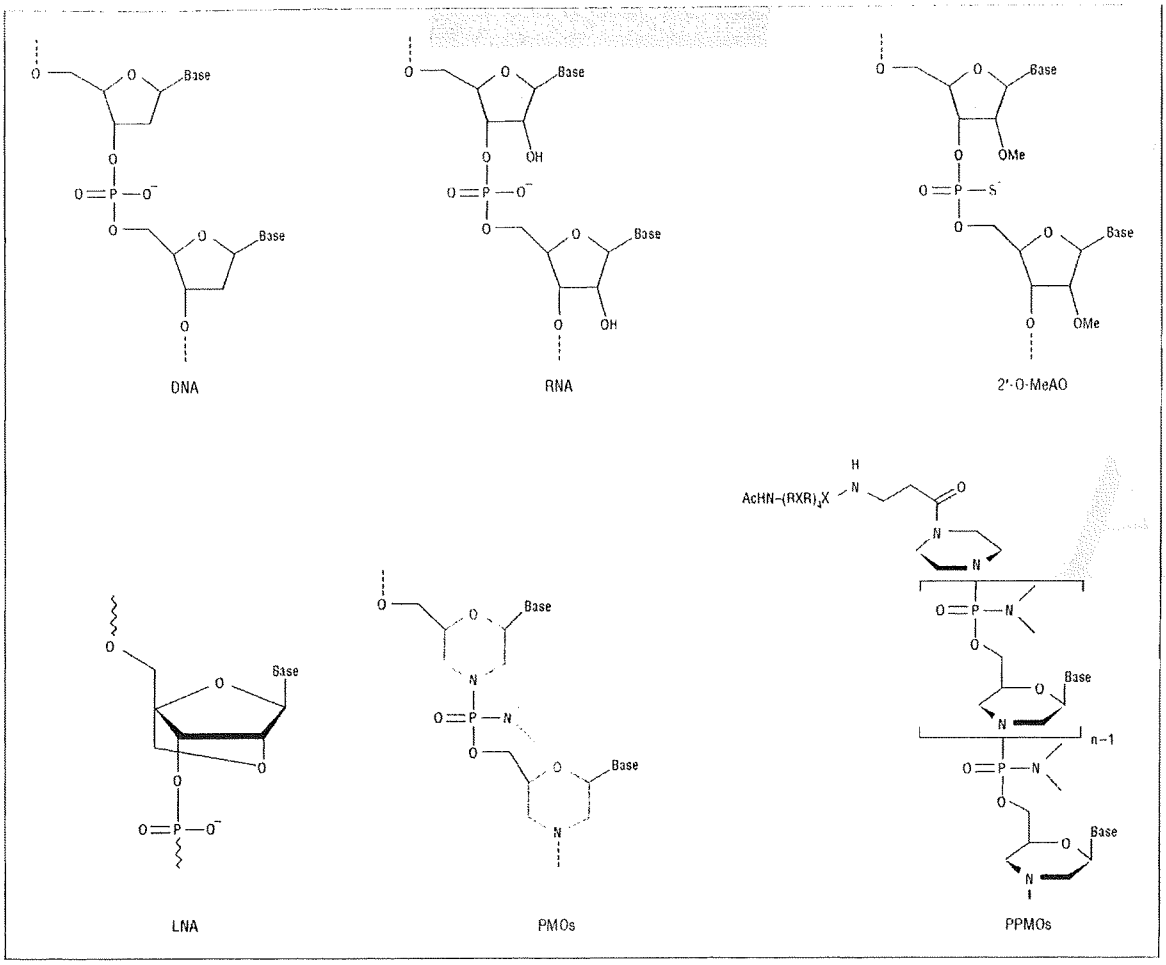

Figure 1. Comparison of chemistries used for the exon-skipping approach. Examples of artificially developed antisense oligomers such as 2'-O-methylated antisense oligonucleotides (2'-O-MeAO) (phosphorothioate), locked nucleic acid (LNA), phosphorodiamidate morpholino oligomers (PMOs), and peptide-tagged PMOs (PPMOs) are shown for comparison with DNA and RNA.

Administration (FDA), fomivirsen sodium (Vitravene; Isis Pharmaceuticals, Inc) delivered by intravitreous injection to inhibit cytomegalovirus retinitis in AIDS. Vitravene was approved in 1998 and there have been no subsequent successful approvals in the ensuing 10 years.

What has slowed the progress of AO drugs into the clinical arena, and why may this be changing?

There have been 2 major hurdles: off-target toxic effects and potency or delivery. Regarding toxic effects, most organisms do not take kindly to covert infiltration by foreign DNA or RNA. Indeed, all species have quite effective mechanisms to destroy foreign DNA and RNA as they are more likely than not to be viruses or other undesirable organisms. In addition, many of the clinical trials testing AO drugs have seen evidence of activation of the complement cascade, and this has been a key concern of the FDA. Delivery has also been a consistent problem. Because the target RNAs are always intracellular, it is imperative for the AO drug to achieve intracellular concentrations sufficient to enable it to bind and modulate the target RNA to a significant extent. The fact that AOs typically do not easily cross the lipid bilayers that bound the cell so as to achieve sufficient intracellular potency via systemic (intravenous) delivery has been problematic.

Recent developments are achieving success in overcoming both hurdles. Analogues of nucleic acid have been designed and synthesized in which the ribose backbone of RNA and DNA is replaced with different chemistries (**Figure 1**). Two are particularly promising: one uses a morpholino backbone (phosphorodiamidate morpholino oligomer [PMO]; AVI BioPharma, Portland, Oregon), and the second uses a locked nucleic acid backbone (Enzon Pharmaceuticals, Inc, Bridgewater, New Jersey). These new backbones are designed to maintain the molecular distance between bases (G, A, T/U, and C), enabling highly sequence-specific base pairing to the target RNA that is stronger in the case of PMO and locked nucleic acid drugs than DNA or RNA AOs. Equally important, these backbones are so dissimilar from the DNA and RNA ribose phosphodiester backbone that they are not recognized by most or any DNA and RNA binding proteins or degrading enzymes, thereby enhancing their stability and avoiding many or all off-target toxic effects.

The second major barrier has been achieving sufficient intracellular concentrations (delivery). One successful approach is to take advantage of preexisting holes in the plasma membrane of the target cell. Infecting viruses breach the cell membrane during the process of infection and appear to bring along AO drugs in the process. As such, AOs have been quite successful in blocking downstream viral replication within cells, and PMO drugs are showing impressive promise as antiviral antidotes.[5] Another preexisting hole is found in muscle cells lacking dystrophin (Duchenne muscular dystrophy [DMD]).[6] The unstable plasma membrane of myofibers appears to allow the AO to leak into the cell.[7] An additional approach is to modify the AO drugs with cell delivery moieties, chemical adducts that penetrate the cell membrane. One example is the addition of arginine-rich peptides to one end of the AO drug (peptide-tagged PMO) (Figure 1).

From these advances has sprung a resurgence of interest in AO drugs for treatment of genetic disease, cancer, and infectious disease. The purpose of most applications is to knock down a target RNA so that it makes less of the deleterious protein product (eg, tumor growth factor β or hypoxia-inducible factor 1α in cancer cells, viral mRNAs, or dominant gain-of-function toxic proteins in inherited neurological disease). However, the disorder that may be most advanced in such applications is DMD. Here the AOs are used for a quite different objective than for previous applications; explicitly, AOs in DMD are designed to restore function to the target mRNA and protein rather than block it. The remainder of this review focuses on this application.

RATIONALE AND PROOF OF PRINCIPLE OF EXON-SKIPPING THERAPY

The principle of exon-skipping therapy for dystrophinopathies was initially demonstrated by Dunckley et al[8] in cultured mouse muscle cells in vitro. The rationale is as follows. Duchenne muscular dystrophy is caused by mutations of the 79-exon gene (commonly deletions of ≥1 exon). Within the myofiber, the remainder of the gene will be transcribed and spliced together. However, if the triplet codon reading frame of the mRNA is not preserved, the resulting frame shift will lead to the failure of dystrophin protein production. Becker muscular dystrophy (BMD) is a clinically milder and more variable disease in which mutations of the dystrophin gene are commonly such as to preserve the translational open reading frame; thus, after splicing together, the remainder of the gene retains some ability to synthesize the dystrophin protein. The goal of exon-skipping therapies is to force the dysfunctional mRNA with out-of-frame mutations in a patient with DMD to skip (exclude) some additional exons. The loss of additional material directed by AO drugs restores the reading frame, changing a Duchenne out-of-frame transcript to a Becker in-frame transcript. Fortunately, most mutations in the dystrophin gene occur in parts that do not code for functionally essential regions of the protein.

This AO-mediated exon-skipping method has been developed and extensively tested on the dystrophic *mdx* mouse model of DMD. The *mdx* mouse harbors a nonsense mutation in exon 23 that prevents translation beyond this point in the transcript. Both local intramuscular injection and systemic delivery of a single AO targeted against exon 23 in the primary transcript excludes this exon from the mRNA, leaving an in-frame transcript that generates dystrophin expression and produces a degree of functional recovery. Intramuscular and systemic injections of AOs for exon splicing of a dog model of DMD have also been demonstrated with a novel cocktail AO strategy (T.Y., S.T., Q.-L.L., T.A.P., A.N., E.P.H., and Masanori Kobayashi, DVM, unpublished data, 2006-2008). The principle is similarly illustrated in humans; van Deutekom et al[9] reported single-site intramuscular injections of 2′-O-methyl AO chemistry in 4 boys with DMD, showing evidence of de novo dystrophin production at the injection site.

These data demonstrate that the key hurdles of achieving intracellular delivery and avoiding toxic effects can be cleared. A similar strategy is being explored in other diseases such as myotonia, human immunodeficiency virus, and spinal muscular atrophy.[10-12]

HURDLES IN BRINGING EXON SKIPPING TO STANDARD OF CARE

Exon skipping using AO drugs has rapidly emerged as the frontline therapeutic approach for DMD. How soon can we expect exon skipping to reach the neuromuscular clinic and standard of care? This approach is breaking new ground and raising challenges not encountered previously in drug development. Different patients have different mutations, and many AO sequences will need to be designed, tested, and FDA approved. Also, current genotype and phenotype data suggest that there may be good in-frame deletions and not-so-good in-frame deletions; simply restoring the reading frame may not be synonymous with restoring dystrophin protein function. The optimization of dystrophin function will likely require deletions of multiple exons, and this will require mixtures of different AOs—new territory for drug development and the FDA. The approach will require regular injections of large amounts of AO drug; what are the long-term toxic effects? Moreover, are the standard toxicity tests appropriate for sequence-specific drugs? Each of these hurdles is discussed briefly in the remainder of this review.

CERTAIN EXON DELETIONS MAY RETAIN MORE DYSTROPHIN FUNCTION THAN OTHERS

The molecular diagnostics of DMD and BMD frequently refer to the reading frame rule, where out-of-frame deletions are given a DMD diagnosis and in-frame deletions are given a BMD diagnosis. However, as many as 30% of patients with BMD do not adhere to this rule.[13] A thorough understanding of reading frames is critical for appropriate design of exon-skipping therapies, both so that the best AO can be given to the patient and so that an optimally functional dystrophin protein is produced as a result of the expected exon skipping. Currently, the best information from which to predict the capabilities of partially deleted dystrophins to rescue the DMD phenotype comes from analysis of the thousands of geno-

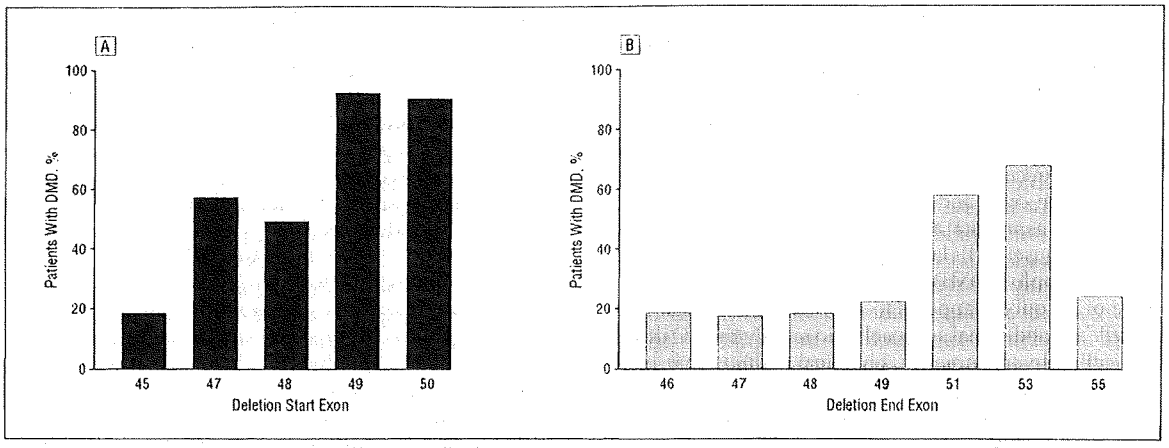

Figure 2. Clinical phenotypes associated with specific start (A) and end (B) sites for in-frame deletions. Percentages of patients with Duchenne muscular dystrophy (DMD) out of patients with DMD or Becker muscular dystrophy with specific start and end exons are shown. Combined muscular dystrophy databases of 14 countries (from Argentina, Belgium, Brazil, Bulgaria, Canada, China, Denmark, France, India, Italy, Japan, The Netherlands, the United Kingdom, and the United States) at Leiden University (http://www.dmd.nl), where diagnoses were performed using multiplex ligation-dependent probe amplification/multiplex amplification and probe hybridization, Southern blotting, or polymerase chain reaction primer sets that allow deletion boundaries to be assigned accurately to a specific exon, are used (deletion start sites: n=288 for exon 45, n=23 for exon 47, n=9 for exon 48, n=12 for exon 49, and n=10 for exon 50; deletion end sites: n=11 for exon 46, n=115 for exon 47, n=95 for exon 48, n=51 for exon 49, n=53 for exon 51, n=40 for exon 53, and n=21 for exon 55).

type and phenotype correlations in patients with DMD and BMD that have been published in the literature and on the Internet. We examined all in-frame deletions and determined the proportion of observed cases that showed mild or severe phenotypes. This was gleaned from combined muscular dystrophy databases of 14 countries (from Argentina, Belgium, Brazil, Bulgaria, Canada, China, Denmark, France, India, Italy, Japan, The Netherlands, the United Kingdom, and the United States) at Leiden University (http://www.dmd.nl), excluding diagnoses that did not allow deletion boundaries to be assigned accurately to a specific exon.[14] Of all observed in-frame deletion patterns on genomic DNA in the central rod domain hotspot region (exons 42-57; 28 distinct patterns), 57% (16 of 28 patterns) were associated with DMD rather than BMD. This analysis showed that there are considerable discrepancies between population-based ratios and pattern-based proportions of severe DMD vs mild BMD phenotypes, and interestingly, the ratio of DMD to BMD remarkably varies between specific deletion patterns. For example, in-frame deletions starting or ending around exon 50 or 51 that encode the hinge region were most commonly associated with severe phenotypes (**Figure 2**) (eg, deletions at exons 47-51, 48-51, and 49-53 are all reported to be associated with a severe DMD phenotype rather than BMD).[15,16]

Two questions arise. First, why do specific patterns of in-frame mutations tend to result in a severe DMD phenotype in contradiction to the reading frame rule? Second, why do different individuals with the same exonic deletion pattern exhibit such different clinical phenotypes? Likely contributory factors include the following: the effect of the specific deletion breakpoints on mRNA splicing efficiency and/or patterns; translation or transcription efficiency after genome rearrangement; and stability or function of the truncated protein structure. The mechanisms controlling accurate splicing of the 79-exon, 2.4 million–base pair dystrophin gene are clearly complex. Introns of the dystrophin gene are highly variable in size, and it is likely that exonic splicing does not take place in an ordered 5′ to 3′ sequence. A complication in interpreting genotype and phenotype correlations is that the deletion in genomic DNA does not always correspond to the material missing from the resulting mRNA. We and others have shown that even in the absence of AOs, a patient may produce 1 or more transcripts that skip additional exons present in the genomic DNA, in effect performing their own private exon skipping.[13] Disruption of splice site information (such as an intervening sequence) in some patients with in-frame gene deletions may cause skipping of additional exons at mRNA splicing, thus leading to out-of-frame transcripts from an in-frame genomic DNA deletion as Kesari et al[13] have recently described. As Menhart[17] has pointed out, it is also likely that quasi-dystrophin variants in the rod domain may show different stability or function because of different types of derangement of spectrinlike repeat domains. Not enough is known about dystrophin structure and function, and the relative importance of the protein sequence within the rod domain remains entirely a matter of speculation. Historically, lack of dystrophin expression has been used as the key criterion for DMD diagnosis. This together with the presence of the DMD clinical picture with such in-frame mutations argues that other confounding variables such as imprecisely defined mutation or aberrant splicing may explain these "exceptions to the reading frame rule." Thus, it is anticipated that most or all patients with mutations in the central rod domain would benefit from the production of truncated dystrophin.

PARALLELING AO TRIALS: TESTING NEW EXONS AND MIXTURES

Clinical proof-of-concept trials testing limited intramuscular injection with a 2′-O-methyl AO against exon 51

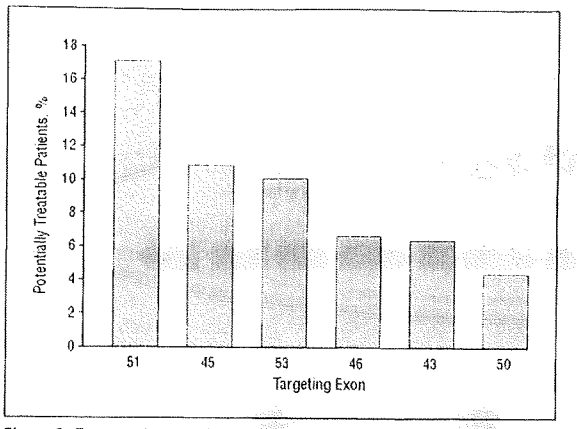

Figure 3. Targets of exon skipping and population of potentially treatable patients. Percentage of patients with the dystrophin deletion who are potentially treatable by targeting specific exons for Duchenne muscular dystrophy. For example, 17% of patients with Duchenne muscular dystrophy who have the dystrophin deletion can be potentially treated by targeting exon 51 using antisense oligonucleotides.

have been published,[9] and similar studies with PMO chemistry are under way in the United Kingdom. Given the many questions concerning the sequence specificity of toxic effects and the large number of AO sequences that will need to be developed as drugs to treat most patients with DMD, it is critical to parallel studies on many more AOs for DMD (**Figure 3**).

It should be noted that about 30% of patients with DMD have nondeletion mutations (duplication, nonsense mutations, small rearrangement, or splice site mutations). Most mutations are theoretically amenable to exon skipping; however, there are no hot spots for point mutations, so relatively few patients would be treatable with each targeted exon by comparison with deletion mutations. Moreover, if skipped to remove a nonsense mutation, the exons that are candidates to restore the reading frame in patients with deletions (eg, exons 43, 45, 46, 50, 51, and 53) will require additional deletion of at least 1 further exon to restore the reading frame because these are frame-shifting exons. Thus, only 35% of nonsense mutations are potentially treatable by single-exon targeting, but the combined data of the Leiden DMD mutation database imply that more than 90% could be responsive to multiskipping.[14]

Development of exonic cocktails (mixtures) could resolve a number of problems, including optimization of dystrophin function and covering relatively high proportions of patients with DMD with a single mixture. The mixture approach has clear advantages and disadvantages. As an example, an 11-exon AO cocktail skipping exons 45 through 55 is predicted to result in a particularly mild BMD phenotype (94% of reported patients).[14] Encouragingly, this large deletion is regularly associated with clinically milder phenotypes than any of the smaller in-frame deletions within the same range of exons 45 to 55.[18] A second advantage is that the cocktail could conceivably be approved as a single drug for most patients with DMD who have dystrophin deletions, independent of their precise deletion, eg, an 11-exon AO cocktail targeting exons 45 through 55 is potentially applicable to more than 60% of patients with a dystrophin deletion (**Figure 4**).[18,19] In total, more than 90% of patients with DMD could potentially be treated by multiskipping, whereas single-exon skipping could treat around half of the patients with dystrophin deletions and point mutations. Systemic studies in the large dog model of DMD have been done using a 3-exon PMO cocktail, and this has clearly been shown to be efficacious by multiple clinical, imaging, histological, and biochemical or molecular end points (T.Y., S.T., Q.-L.L., T.A.P., A.N., E.P.H., and Masanori Kobayashi, DVM, unpublished data, 2006-2008).

A disadvantage of the cocktail approach is the addition of novel hurdles for FDA or regulatory approval. Current FDA regulations require each component of a drug mixture to undergo toxicological and clinical testing and then require the mixture to similarly undergo toxicological and clinical testing. In the context of an ideal 11-exon AO cocktail, the regulatory barriers become truly intimidating. In addition, the 11-exon cocktail PMO approach would lead to delivery of some AOs that may not have a target in a specific patient (eg, the patient already has a deletion of ≥1 exon in the AO mix). Thus, some parts of the mixture will have no possible potential molecular or clinical benefit to individual patients. This would again be uncharted territory for the FDA. While clinical development of the 11-exon mixture is likely ambitious at present, it will be important to initiate toxicological and clinical trials of exon mixtures for subsets of patients who cannot be treated with a single AO. Also, for future trials on multiskipping such as with exons 45 through 55, we should have as many AOs in hand as possible because they can be used as part of multiskipping AOs.

PERSONALIZED MEDICINE AND THE FDA: ARE EXISTING GUIDELINES APPROPRIATE?

Personalized medicine has many definitions, but most share the concept of optimizing a treatment for a particular patient. Designing and using AO drugs targeted for a patient's specific gene mutation would seem to fit well within this rubric. As such, the promising AO exon-skipping approach may bring neuromuscular disease to the frontline in development of drugs for personalized medicine. It is important to examine the existing FDA guidelines for drug development and reinterpret these guidelines in the context of AO and DMD. For example, the drug development pipeline includes phase 1 studies of the drug in healthy volunteers. However, successful on-target exon skipping of the dystrophin gene in healthy volunteers would give them DMD, a clear adverse effect that is entirely irrelevant to toxic effects in the target patient population (boys with DMD). Toxicity tests are currently done in animal models (typically 2 species), but one of the major concerns regarding toxic effects of AO drugs is binding to off-target RNAs. For example, if an AO drug designed for exon skipping of the dystrophin mRNA also binds to the closely related utrophin mRNA, then exon skipping of utrophin might occur and could result in off-target adverse effects. The utrophin sequence of mice or rats is different from the utrophin sequence of humans, so the standard rodent toxicity tests